9950-1356
P-70

SHUTTLE DATA BOOK
SRM FRAGMENT VELOCITY MODEL

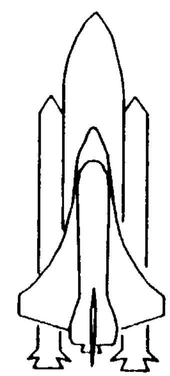

PRESENTED TO THE
SRB FRAGMENT MODEL REVIEW PANEL

This report was prepared for the Jet Propulsion Laboratory, California Institute of Technology, sponsored by the National Aeronautics and Space Administration.

2 MARCH 1989
NASA HEADQUARTERS
WASHINGTON, D.C.

BRIEFER:
M.B. ECK

INTRODUCTION

- THE STUDY DESCRIBED IN THIS BRIEFING WAS UNDERTAKEN TO DETERMINE THE VELOCITY OF FRAGMENTS GENERATED BY THE RANGE SAFETY DESTRUCTION (RSD) OR RANDOM FAILURE OF A SPACE TRANSPORTATION SYSTEM (STS) SOLID ROCKET MOTOR (SRM).

- LARGE, HIGH VELOCITY SRM FRAGMENTS WERE OBSERVED TO HAVE BEEN GENERATED IN THE STS-51L (CHALLENGER) EVENT.

- THE SPECIFIC REQUIREMENT OF THIS STUDY WAS TO PROVIDE A FRAGMENT MODEL FOR USE IN THOSE GALILEO AND ULYSSES RTG SAFETY ANALYSES CONCERNED WITH POSSIBLE FRAGMENT IMPACT ON THE SPACECRAFT RADIOISOTOPE THERMOELECTRIC GENERATORS (RTGS).

  THIS MORNING'S BRIEFING IS DIVIDED INTO TWO MAJOR SECTIONS:

  - MODEL DEVELOPMENT AND APPLICATION

  - MODEL REVIEW AND BOUNDARY ASSUMPTION VERIFICATION

- A CRITIQUE OF AN SRM FRAGMENT VELOCITY MODEL DEVELOPED BY PERSONNEL AT THE NAVAL SURFACE WARFARE CENTER (NSWC) WILL BE THE SUBJECT OF THIS AFTERNOON'S BRIEFING.

RTG LOCATIONS FOR GALILEO AND ULYSSES SPACECRAFT LAUNCH BY SPACE SHUTTLE

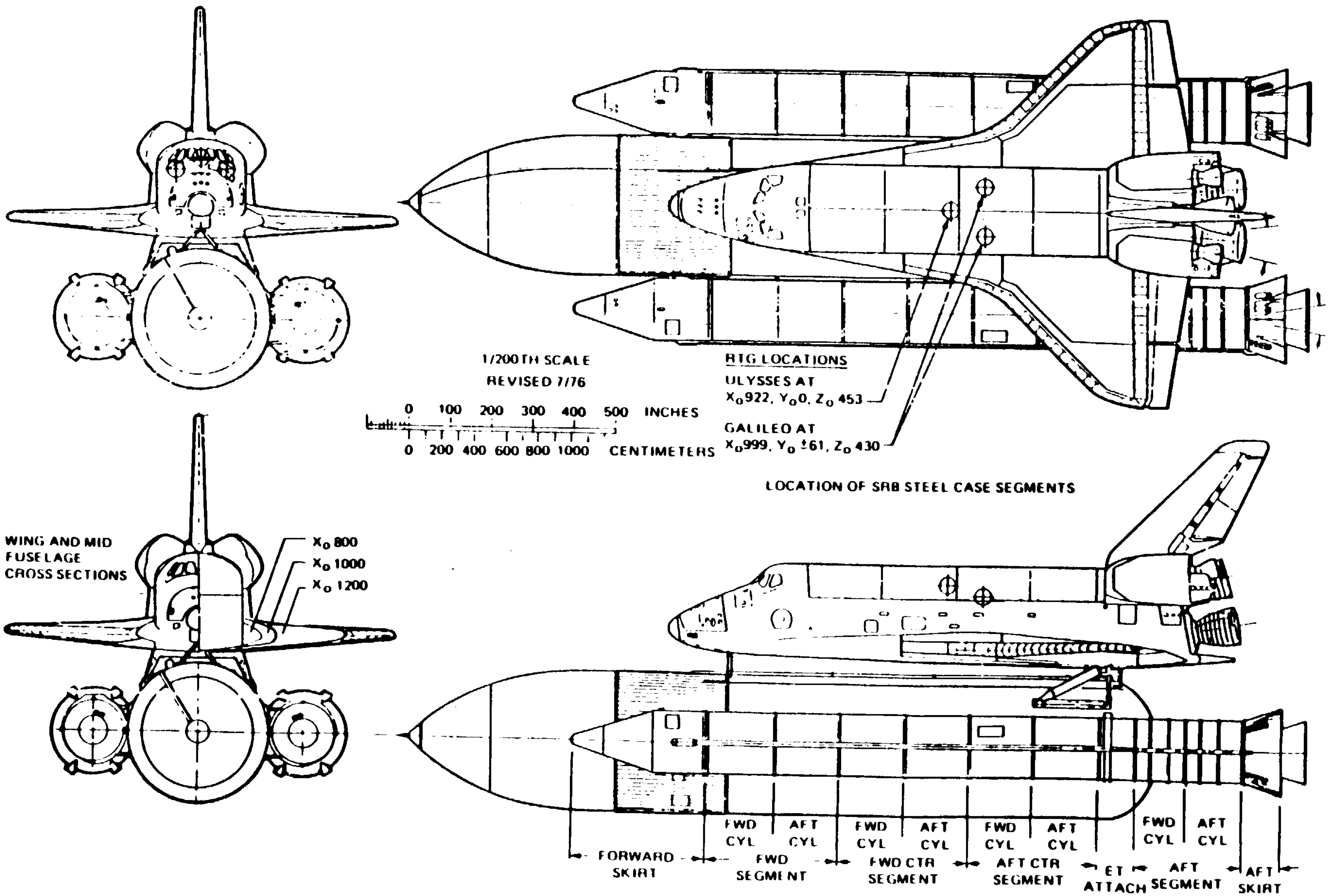

INTRODUCTION (CONT'D)
MORNING BRIEFING ORGANIZATION

I. Model Development and Application	II. Model Review and Boundary Assumption Verification
● What We Did, Why We Did It, and What Resulted. • Study Objectives • Reprise of the Physical Evidence • Physical Evidence Implications • Required Model Attributes • Model Development • Model Results • Comparison of Model Results to Observations	● Sanity Checks-Special Analyses Used to Verify the Original Modeling Approach. • Unit-Length Energy/Mass Ratios • One and Two Chamber Flow Models Using Rigid Body Assumptions • Effects of 3D flow and Fragment Rotation Using Rigid Body Analyses • New, Detailed Model Used to Assess: - PBAN Grain and Bond Strength Effects - PBAN Material Properties: Effects of High Strain Rates - PBAN Crack Initiation and Propagation

S-087 105R 02 89C

STUDY OBJECTIVES

- THE STUDY DESCRIBED IN THIS BRIEFING HAD THE FOLLOWING DETAILED OBJECTIVES:
  - PREDICT SRM FRAGMENT VELOCITY OVER THE ENTIRE MISSION ELAPSED TIME (MET) DOMAIN FOR BOTH RANDOM AND RSD FAILURES.
  - PREDICT SRM FRAGMENT AZIMUTH OVER THE MET RANGE FOR RANDOM AND RSD FAILURES.
  - PREDICT SRM FRAGMENT ROTATION RATE OVER THE MET RANGE FOR RANDOM AND RSD FAILURES.
  - PERFORM A LARGE NUMBER OF PARAMETRIC SENSITIVITY ANALYSES TO DETERMINE THE STATISTICAL DISTRIBUTION OF PROBABLE FRAGMENT ENVIRONMENTS RESULTING FROM STS-SRM RANDOM OR RSD FAILURE.
  - THE RESULTS OBTAINED USING THE METHODS DEVELOPED WERE TO BE CONSISTENT WITH ALL AVAILABLE PHYSICAL EVIDENCE.

REPRISE OF THE SRM FRAGMENT VELOCITY PHYSICAL EVIDENCE

- TWO MAJOR SRM FAILURES OCCURRED IN EARLY 1986:
  - THE STS-51L AT 110 SECONDS MET
  - THE TITAN 34D-9 AT 10 SECONDS MET
- DETAILED STUDIES OF THE FILMS OF THESE EVENTS WERE UNDERTAKEN AS WERE ON-SITE INSPECTION OF ALL REMAINING PHYSICAL EVIDENCE.
- THE FOLLOWING IS AN ANECDOTAL COMPILATION FROM DIRECT PHYSICAL INSPECTION OF THE AVAILABLE EVIDENCE BY THE PARTICIPANTS IN THE MODELING EXERCISE TO BE DESCRIBED.
  - GRAIN (PBAN) DEBONDING WAS A COMMON FEATURE OF ALMOST ALL OF THE 34D-9 FRAGMENTS (EARLY MET FAILURE)
  - GRAIN DEBONDING WAS NOT A COMMON FEATURE OF THE STS-51L FRAGMENTS (LATE MET FAILURE WITH LESS THAN THREE INCHES OF FUEL REMAINING)

REPRISE OF THE SRM FRAGMENT VELOCITY PHYSICAL EVIDENCE (CONT'D)

  - MOST CASING CRACKS ORIGINATED AND ENDED IN CLEVIS PIN HOLES. THIS WAS COMMON TO BOTH THE STS-51L AND 34D-9 EVENTS.

  - FRAGMENTS FROM THE RANDOM FAILED 34D-9 MOTOR (SRM-2) SHOWED A DECREASE IN VELOCITY FROM SEGMENT 1 TO 4 (SEGMENT 1 FAILED FIRST).

- BOTH STS-51L SRMS WERE DESTROYED BY THE INITIATION OF A SINGLE 1000 GRAIN/FOOT HMX LINEAR SHAPED CHARGE (LSC).

- ONE 34D-9 SRM WAS DESTROYED BY THE INITIATION OF TWO 700 GRAIN/FOOT HMX LSCS SPACED TWO INCHES APART. THE OTHER 34D-9 SRM FAILED RANDOMLY IN SEGMENT 1.

- SOME OF THE DETAILED MAPS OF THE POST 34D-9 EVENT FRAGMENT LOCATIONS WHICH WERE PREPARED BY R AND D ASSOCIATES' PERSONNEL ARE PRESENTED IN THE FOLLOWING FOUR VUGRAPHS.

FRAGMENT ORIGIN AND LOCI GENERATED FROM THE RSD OF TITAN 34D-9 SRM1

Composite Loci of Cutline Fragments

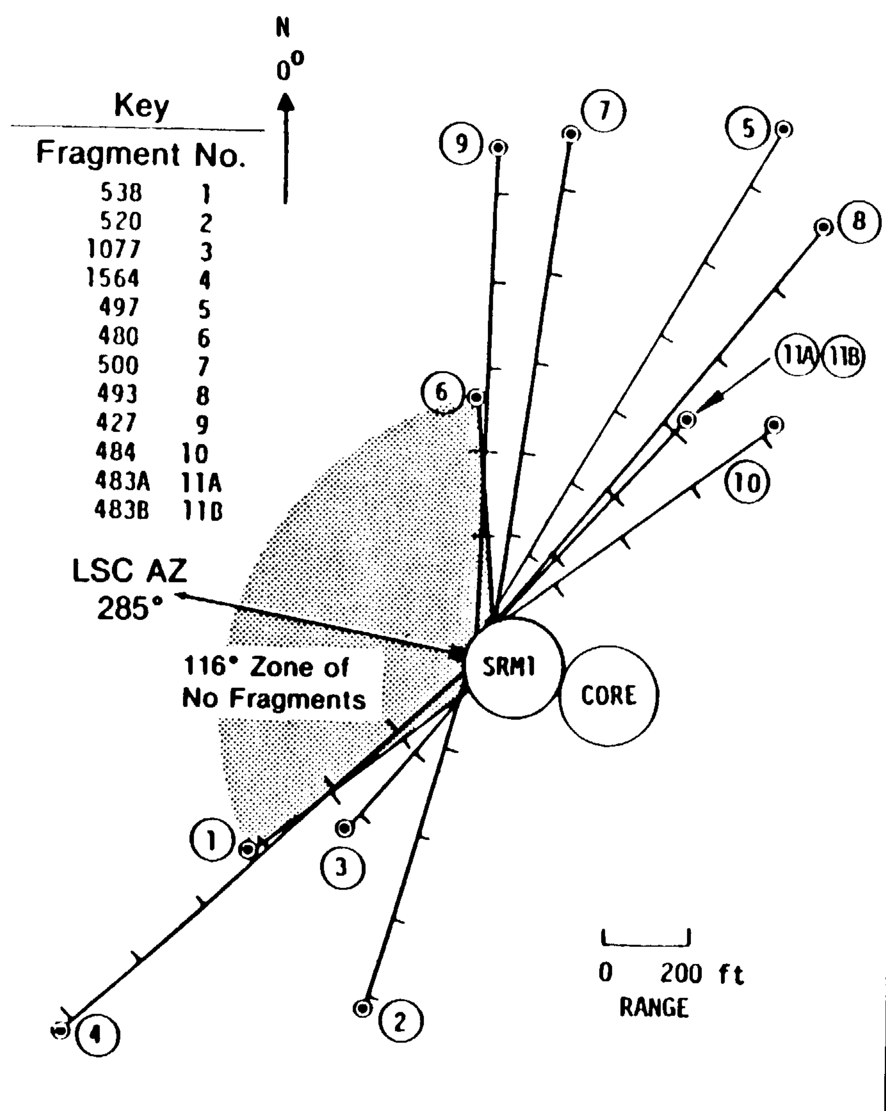

Reconstruction Based on Recovered SRM Fragments

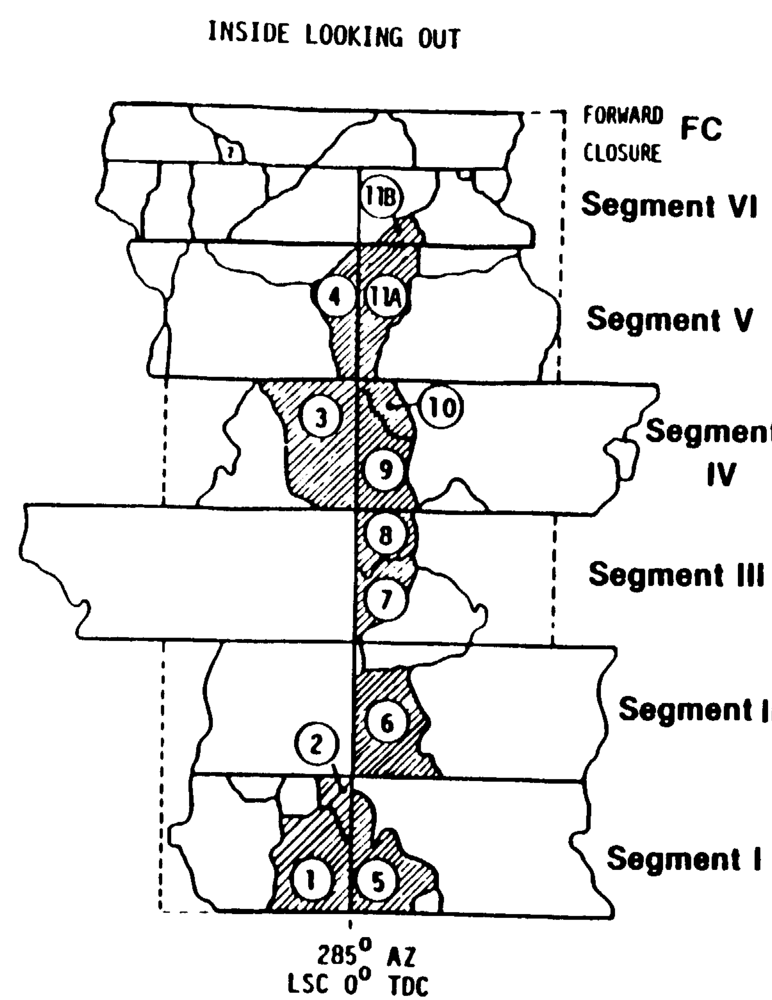

S-087 75R 02-89C

FRAGMENT LOCI GENERATED FROM THE RSD OF TITAN 34D-9 SRM1

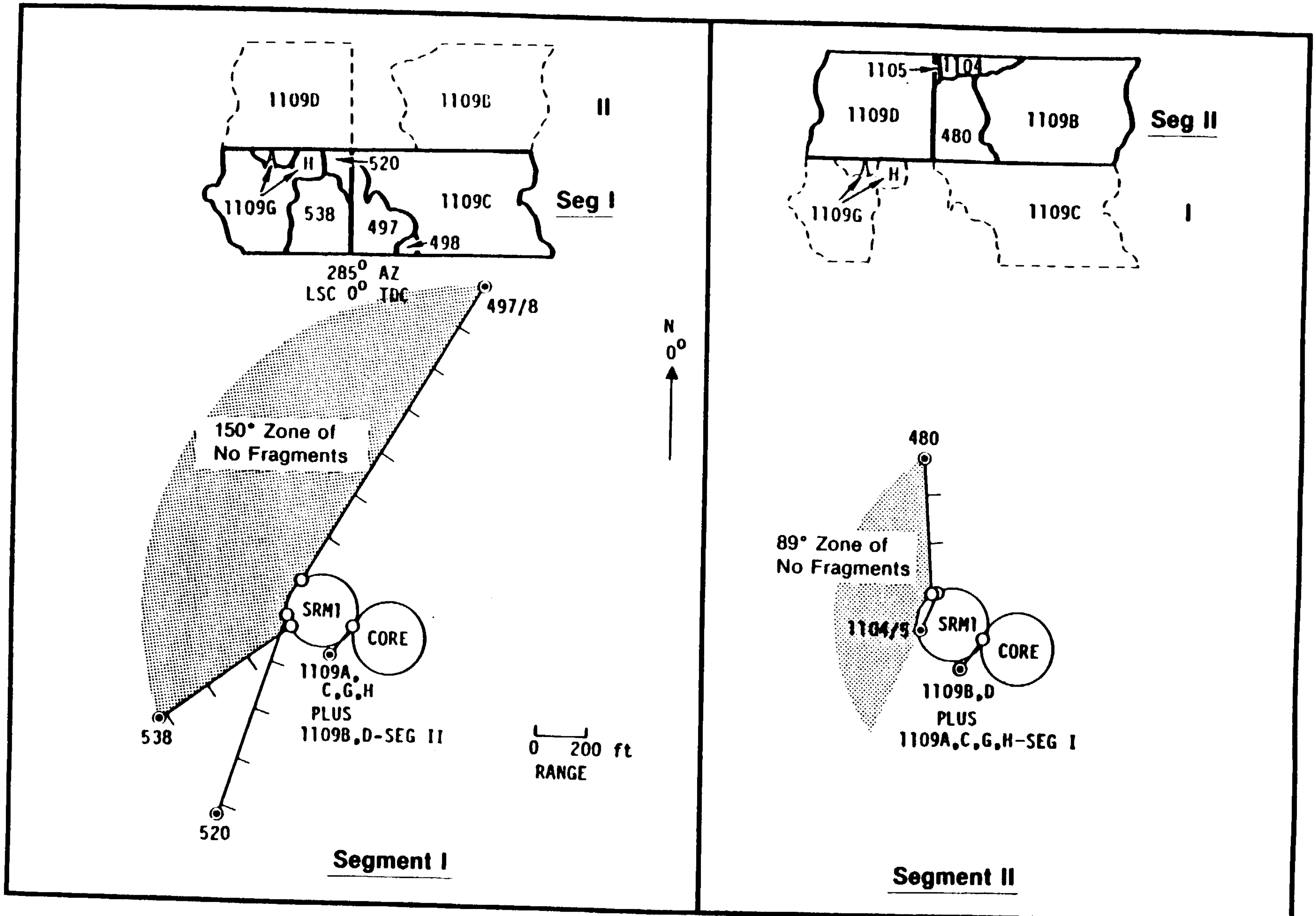

S-087 72R 02-89C

FRAGMENT LOCI GENERATED FROM THE RSD OF TITAN 34D-9 SRM1

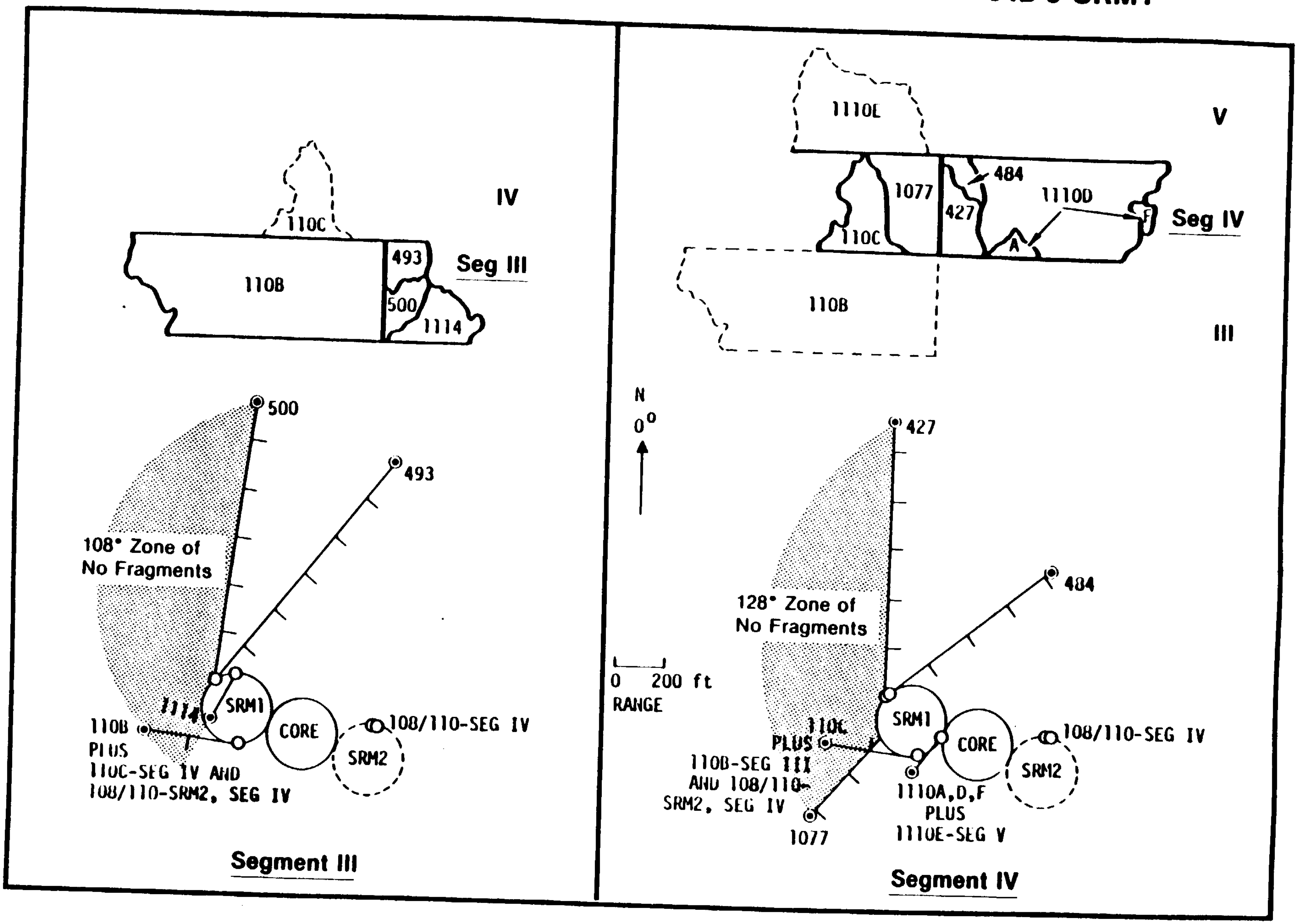

S-087 73R 02-89C

FRAGMENT LOCI GENERATED FROM THE RSD OF TITAN 34D-9 SRM1

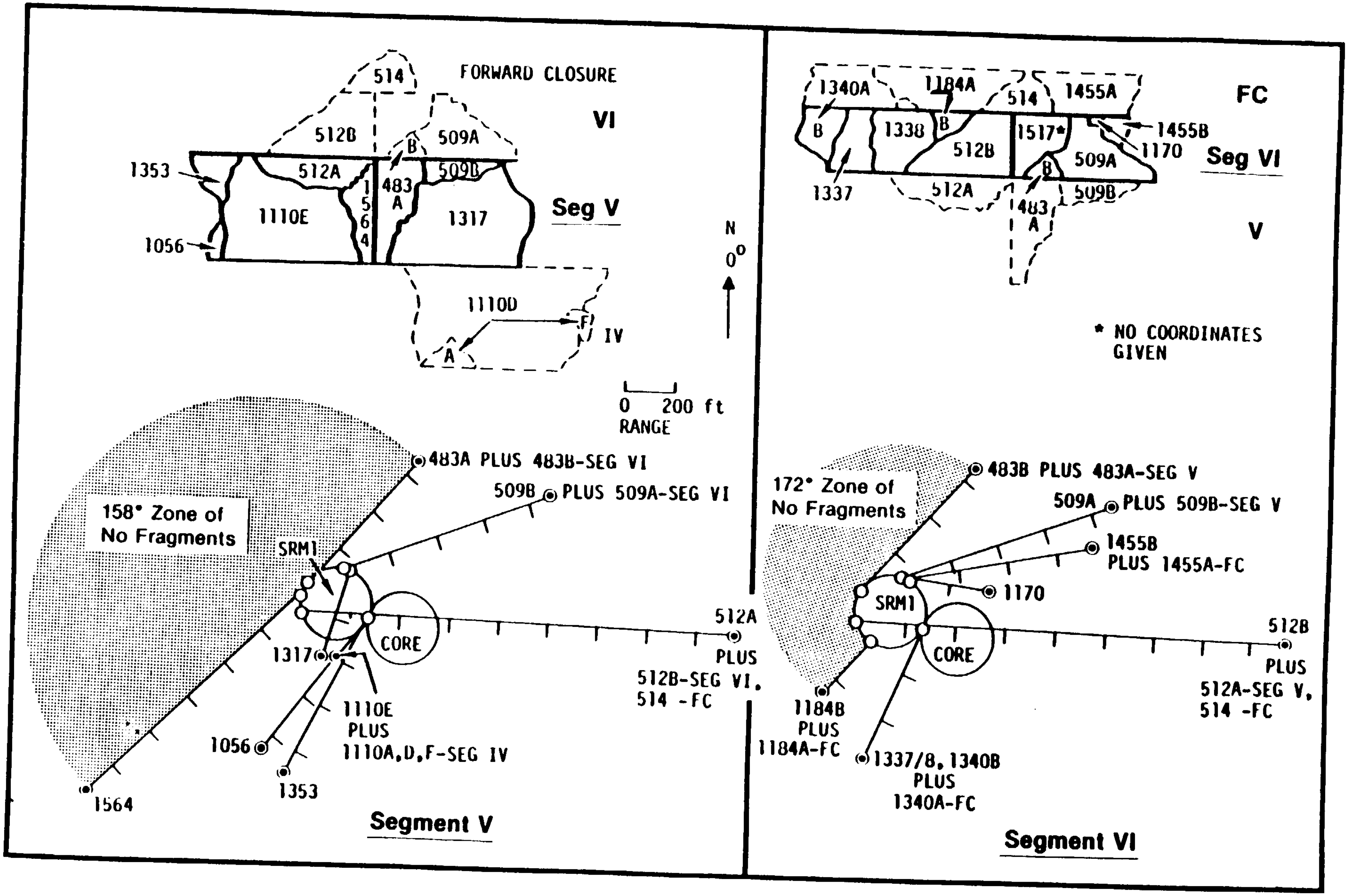

S-08774R 02-89C

TITAN 34D-9 SRM2 FRAGMENT AZIMUTH DISTRIBUTION FOR RANDOM FAILURE - AFTER NANCE

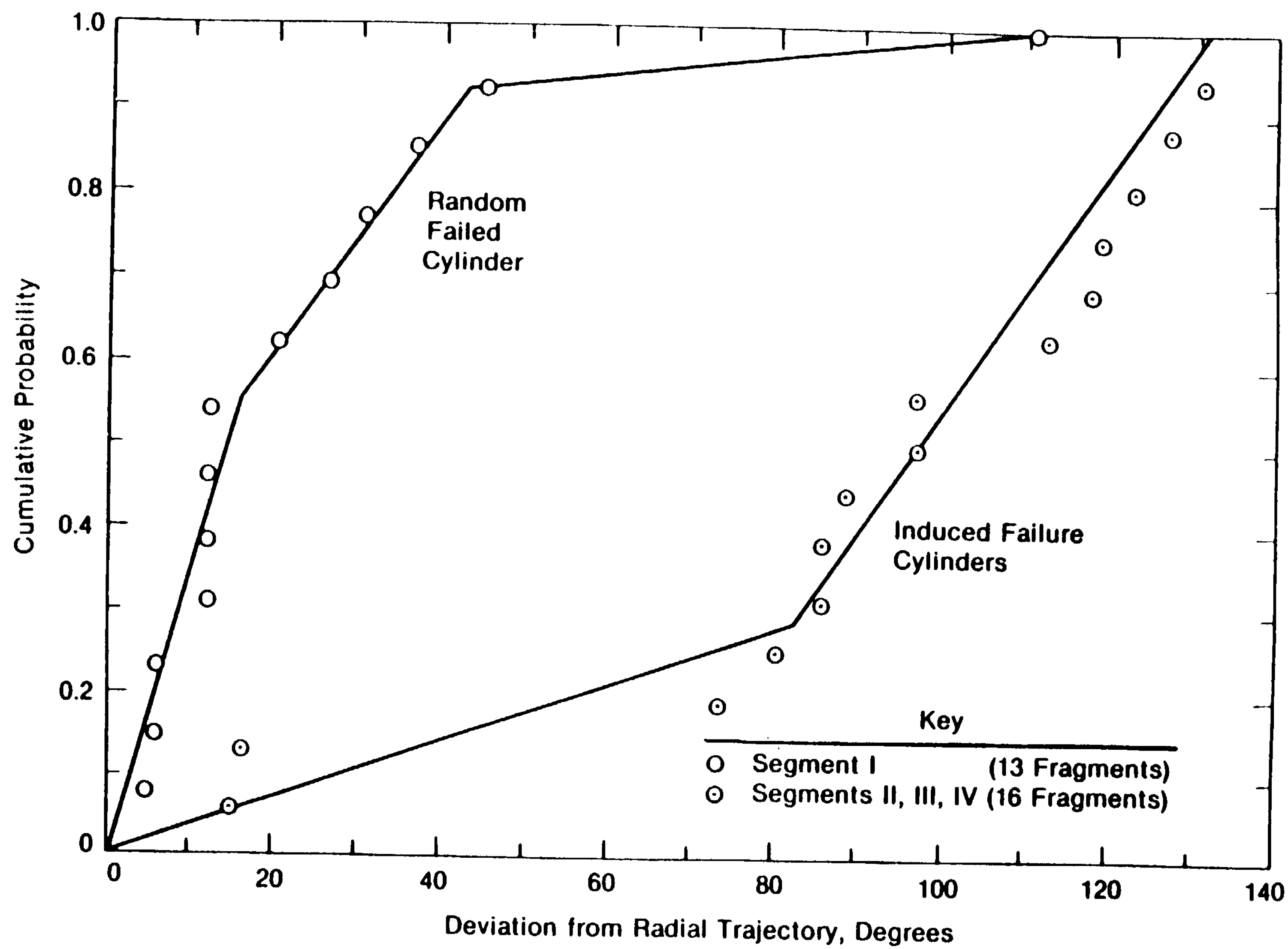

S-087 107R 02-89C

OBSERVED STS-51L FRAGMENT VELOCITIES (1)

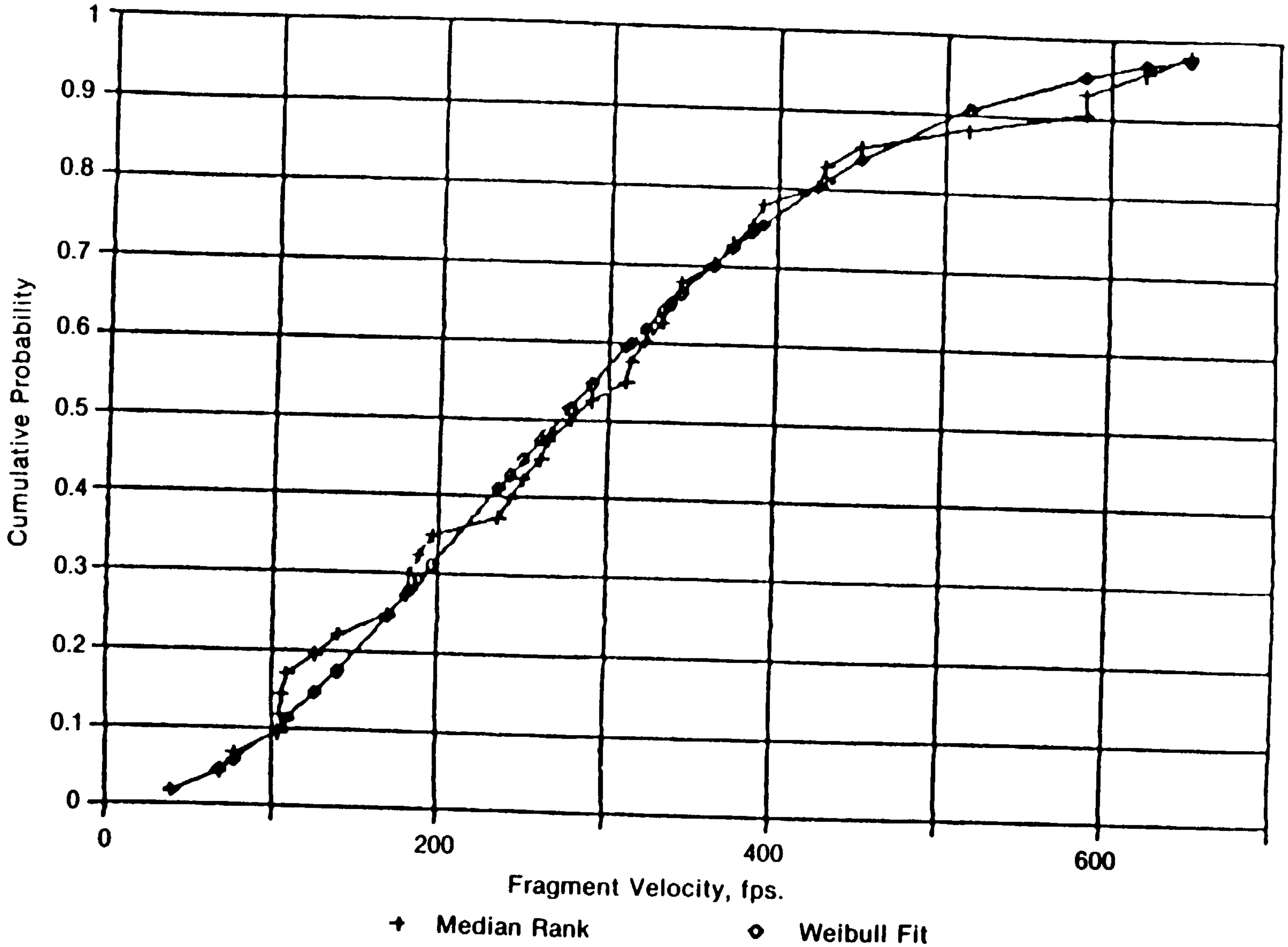

(1) Parker, L., Final Report of the STS 51-L Explosion Working Group (Draft), Section IV, "Solid Rocket Motor Fragmentation Analysis"

S-087.108R 02-89C

IMPLICATIONS OF THE PHYSICAL EVIDENCE STUDY

- TO BE CREDIBLE, ANY MODEL MUST PREDICT THE MAGNITUDE OF THE OBSERVED FRAGMENT ATTRIBUTES WITH A REASONABLE DEGREE OF ACCURACY. THESE ATTRIBUTES INCLUDE:
  - AZIMUTH OF 34D-9 FRAGMENTS
  - VELOCITIES AND VELOCITY DISTRIBUTIONS OF 34D-9 AND 51L FRAGMENTS
  - ROTATION RATES OF 34D-9 AND 51L FRAGMENTS
  - RANDOM FAILURE CASES MUST SHOW A VELOCITY DEPENDENCE WITH LONGITUDINAL POSITION SIMILAR TO THAT OBSERVED IN THE 34D-9 EVENT

- FAILURE TO PREDICT THE SPECTRUM OF FRAGMENT ATTRIBUTES RELIABLY CONSTITUTES A REQUIREMENT TO REVIEW THE ANALYTICAL METHODS AND TO MAKE APPROPRIATE CHANGES UNTIL PREDICTION AND OBSERVATION COME INTO AGREEMENT.

- SINCE THE 34D-9 AND STS-51L EVENTS OCCURRED AT THE EXTREMES OF THE MET RANGE, A SIMILITUDE ARGUMENT MUST BE MADE TO DEVELOP A DATA BASE. THERE IS NO DIRECT OBSERVATIONAL EVIDENCE OF AN RSD ACTION ON A STS-SRM AT 10 SECONDS MET.

REQUIRED MODEL ATTRIBUTES

- THE PISCES CODE VERSION AVAILABLE ACCEPTS MODELS IN 2D TRANSLATIONAL SYMMETRY AND 2D AXISYMMETRY. TO USE THIS CODE, IT MUST BE SHOWN THAT THE EFFECTS OF THE EVENTS OF INTEREST CAN BE ACCURATELY MODELED IN TWO DIMENSIONS.

  - FACTORS IN THIS ASSESSMENT INCLUDED:

    - WAVE TRANSIT TIME REQUIRED TO COMMUNICATE INFORMATION OCCURRING IN ADJACENT SRM SEGMENTS
    - SEGMENT TO SEGMENT FLOW EFFECTS

  - IT WAS CONCLUDED THAT A 2D MODEL WAS ADEQUATE TO MODEL AN RSD ACTION, BUT THERE WAS A NEED TO ACCOUNT FOR LONGITUDINAL FLOW EFFECTS IN RANDOM SRM FAILURE CASES.

- RELATIVE MOVEMENT OF ALL SEGMENT MASSES MUST BE TRACKED THROUGHOUT THE EVENT.

  - COUPLE GAS-DYNAMICS TO MOVEMENT OF GRAIN AND CASING.
  - SOLVE MATERIAL CONSTITUTIVE EQUATIONS, MOMENTUM EQUATIONS AND ENERGY EQUATIONS FOR ALL MODEL CONSTITUENTS SIMULTANEOUSLY.

- THE MODEL MUST PRODUCE RESULTS CONSISTENT WITH THE PHYSICAL EVIDENCE OBTAINED FROM THE 34D-9 AND STS-51L EVENTS.

MODEL DEVELOPMENT

- FOUR SEPARATE MODELS WERE DEVELOPED TO EVALUATE THE VARIOUS MET DEPENDENT SRM FRAGMENTATION MODES. THESE MODELS WERE:
  - EARLY MET 2D TRANSLATIONAL SYMMETRY COUPLED EULER-LAGRANGIAN MODEL FOR BOTH THE STS AND 34D (34D USED IN MODEL VERIFICATION).
  - A LATE MET 2D TRANSLATIONAL SYMMETRY COUPLED EULER-LAGRANGIAN MODEL WITH A PROVISION FOR Z-FLOW INTRODUCTION.
  - A COUPLED EULER-LAGRANGIAN MODEL TO DETERMINE THE SRM LONGITUDINAL PRESSURE DISTRIBUTION EXTANT DURING RANDOM FAILURE.
  - A FAST RUNNING POST PROCESSOR MODEL WHICH WAS USED TO INVESTIGATE PARAMETER SENSITIVITY AND TO DEVELOP A VIABLE FRAGMENT ENVIRONMENT DATA BASE.
- ALL OF THESE MODELS WERE USED IN THE DEVELOPMENT OF THE FRAGMENT ENVIRONMENTS PRESENTED IN THE SHUTTLE DATA BOOK (NSTS-08116).
- EACH OF THESE MODELS WILL BE DISCUSSED IN TURN.

EARLY MET COUPLED EULER-LAGRANGIAN MODEL DESCRIPTION

- A DETAILED COUPLED EULER-LAGRANGIAN 2D TRANSLATIONAL SYMMETRY MODEL WAS DEVELOPED TO DETERMINE EARLY MET HOT GAS AND SRM COMPONENT INTERACTIONS. KEY FEATURES OF THIS MODEL ARE SHOWN IN THE ADJACENT VUGRAPHS.
  - EQUILIBRIUM STORED STRAIN ENERGY WAS ESTABLISHED BY RUNNING A JOINED MODEL UNTIL PROBLEM KINETIC ENERGY WENT TO ZERO.
  - AT THE TIME OF LSC INITIATION OR RANDOM FAILURE THE CASING WAS UNJOINED AT THE ZERO DEGREE LOCATION, THE CASING WAS DEBONDED FROM THE GRAIN, AND THE GRAIN WAS FRACTURED BETWEEN THE SUBGRIDS.
  - A LIP WAS INTRODUCED INTO THE HIGH VELOCITY GAS ISSUING FROM CRACKS IN THE GRAIN. THE PURPOSE OF THIS LIP WAS TO PROVIDE A MEANS TO PRESSURIZE THE CASE-GRAIN CAVITY.
  - TYPICAL FLOW FIELD RESPONSES ARE SHOWN AS A FUNCTION OF TIME IN THE ADJACENT VUGRAPH. THE LIP IS A COMPUTATIONAL CONVENIENCE WHICH HAS CAUSED CONSIDERABLE CONFUSION. IT WILL BE EXPANDED UPON SHORTLY.

SUMMARY OF SRM FRAGMENT MODEL FEATURES

Model Rationale	Model Features

• Grain (PBAN) Plays a Major Role in Fragment Velocity Behavior at Early MET
• Properties of PBAN Under Dynamic Loading Are Not Well Known. (1)
• It was Postulated that the Only Reliable Way to Model SRM Fragmentation was to Predict the Behavior of the 34D-9 Event in Detail, Make a Macro Calibration of the Material Properties and Methods Used and Devise a Method of Generalizing the Observed Fragment Velocity Distribution.
• SRM Failure Occurred in a Time Domain Only a Few Percent of the First Mode of the 34D-SRM. It was reasoned that Wave Interactions Were Important and a Hydrocode Should Be Used to Exercise the Model.
• Also Because of Wave Transit Time Considerations, It Was Assumed that Translational Symmetry Arguments Were Adequate for the Component Motion Analyses.
 	
(1) Moore, C. SRM Propellant and Polymer Materials Structural Test Program. Marshall Space Flight Center, Alabama, March, 1988.
	• Fully Dynamic
	  • Constitutive Equations, Energy Equations and Equations of Motion Solved Simultaneously Using Explicit-Finite-Difference Techniques
	  • Gas Dynamics Coupled to the Casing and Grain Motions
	• 2-D Translational Symmetry Used for Component Motions
	  • No Influence on Segment of Interest by Adjacent Segments is Assumed
	• 2-D Axisymmetry Used for Gas Dynamics
	  • Longitudinal Chamber Flow Must be Considered in Random Failure Case
	• Non-Radial Trajectory
	  • Casing Fragment's Trajectory Predicted Based on Assumed Range of Casing Fragmentation Times
	• Rotation Rates Predicted
	• Fragment Velocity Distribution Predicted
	  • Predicted Results Were Matched to 34D-9 Results by Assumption of an Effective-Pressure Reduction Factor (Kp)
	  • A Similitude Argument was Used for STS Velocity Distribution Predictions

S-087 109 02-89C

34D-9 MODEL INITIAL GEOMETRY SHOWING GRAIN SLIDELINE LOCATIONS

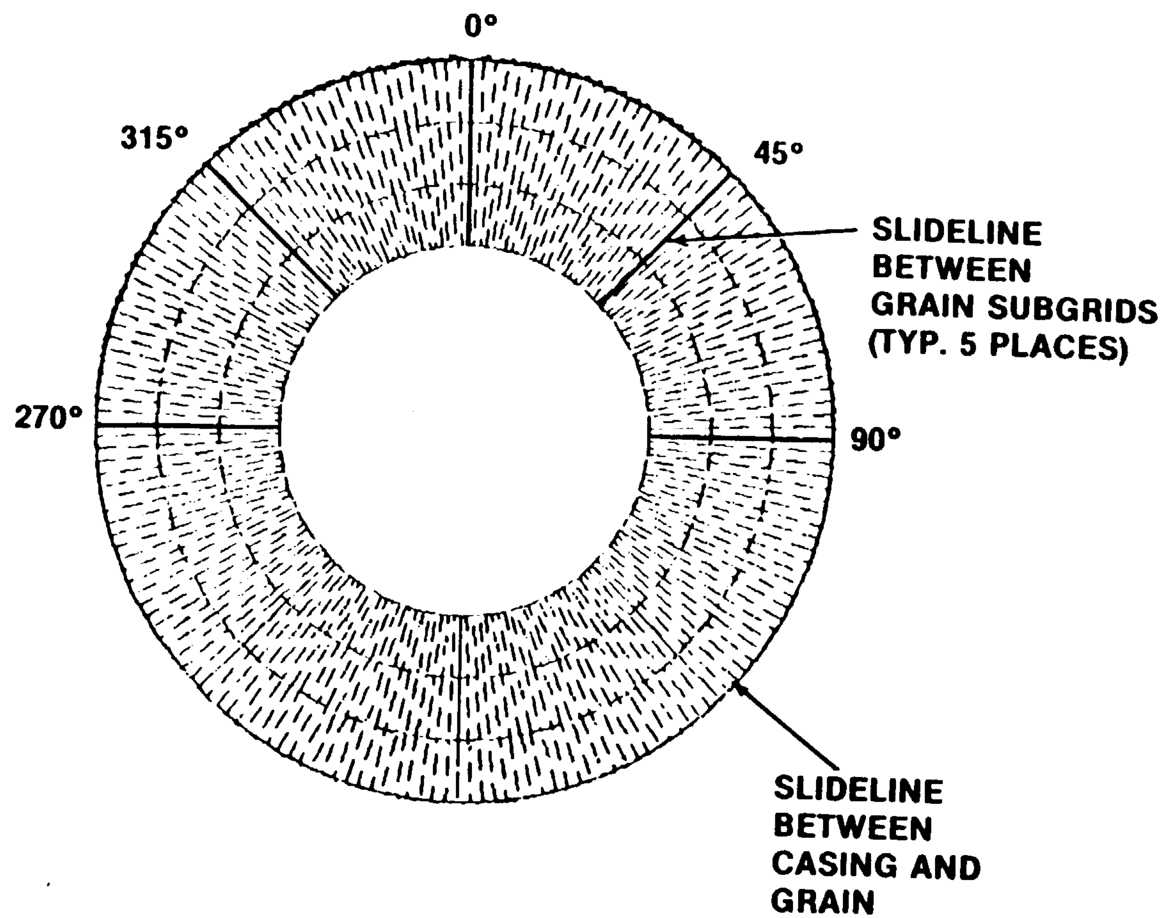

SUMMARY OF MATERIAL CONSTITUTIVE PROPERTIES AND MODELS USED IN THE SHUTTLE DATA BOOK SRM FRAGMENT VELOCITY MODEL

Material	Equation of State			Yield Model			Data Source
	Type	Bulk Modulus KBAR	Reference Density gm/cc	Type	Shear Modulus KBAR	Yield Strength KBAR	
Casing Steel, D6A	Poly.	1670	7.86	Von Mises	816	12.9	Ladish Data Sheet FSCM #07703 (1987)
Grain, PBAN							
Low Strain Rate (< 200/Min)	Poly. (a)	33.5	1.775 (b)	Von Mises	.0403	48.3	Backlund, Stan. Personal Communication. United Tech. Corp. Oct. 1987.
High Strain Rate (1800/Min)	Poly. (a)	143	1.775 (b)	Von Mises	.172	48.3	Clayton, R. Personal Communication. Jet Prop. Lab. Jan. 1989.(d)
Grain Reaction Gas	γ,1.142	-	0.00571 (c)	Specific Internal Energy = 6.72E 10 Ergs/gm			NSWC TR 80-417

(a) The Thiokol Prony Model Could Have Been Mechanized Within the Pisces Code to Model Visco-Elastic Effects. It was Felt that this Refinement was not Justified Because of the Large Uncertainty in the Behavior of PBAN Under Destructive Disassembly Loading.

(b) The Rubber Insulator is Treated as Having the Same Physical Response as the Grain. The PBAN is Adjusted from 1.76 GM/CC to Account for the Presence of the Insulation.

(c) Varies with Burn Time. See FSC-ESD-217-88-426, Table 5 for Details.

(d) Based on Work by C. Moore, Reported in SRM Propellant and Polymer Materials Structural Test Program. Marshall Space Flight Center, Alabama, March, 1988.

EARLY MET COUPLED EULER-LAGRANGIAN MODEL DESCRIPTION (CONT'D)

  - A SERIES OF CONTOUR PLOTS OF THE PRESSURE WITHIN THE CAVITY WAS PREPARED.

  - THE AVERAGE PRESSURE ACTING ON THE CASING WAS DETERMINED FROM THESE CONTOUR PLOTS AS A FUNCTION OF TIME.

  - THE GEOMETRIC RESPONSE OF THE VARIOUS CONTINUA WERE RECORDED.

- THIS DETAILED MODEL WAS USED TO PREDICT THE RESPONSE OF BOTH THE 34D-9-SRM AND THE STS-SRM AT 10 SECONDS MET. ADDITIONAL COUPLED CALCULATIONS WERE PERFORMED AT LATER MET.

DEVELOPING FLOW FIELD IN THE GRAIN - CASING CAVITY AT VARIOUS TIMES AFTER A 34-D SRM CASING FAILURE AT 10sec MET

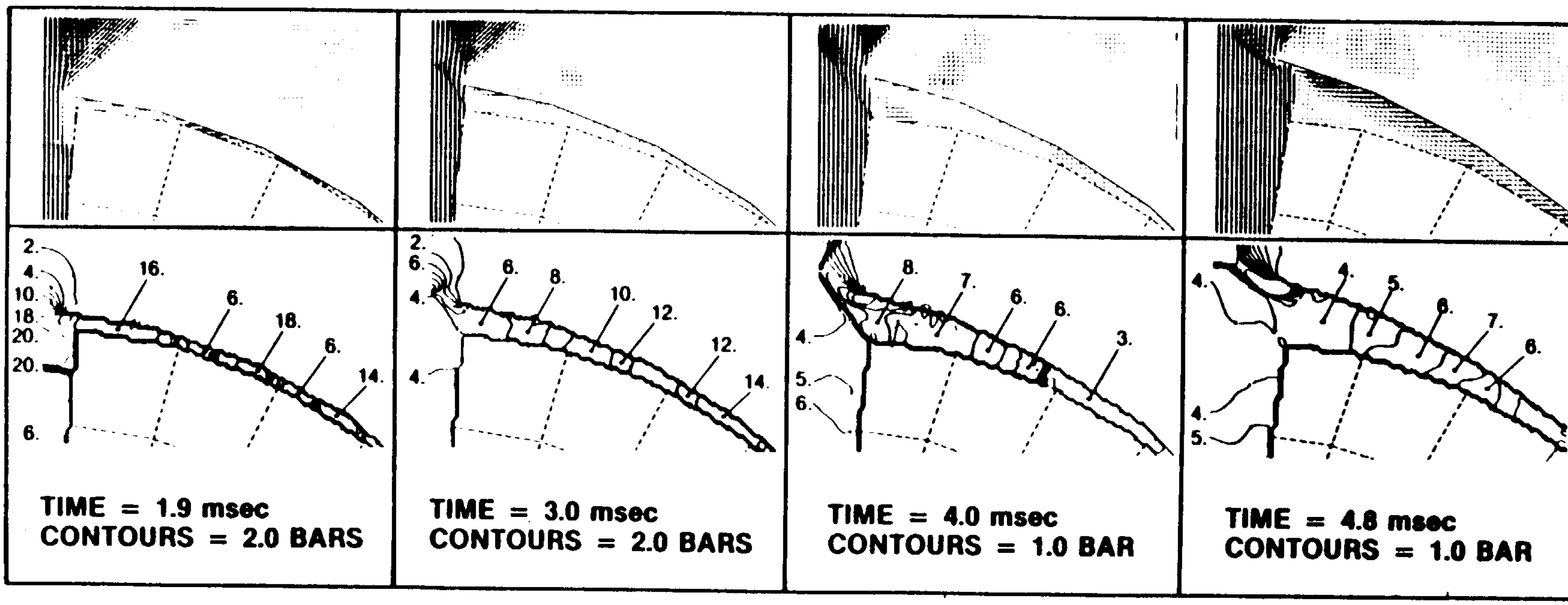

CAVITY PRESSURIZATION

- THE ADJACENT VUGRAPH SHOWS THE GENERAL BEHAVIOR OF AN SRM AS IT UNDERGOES DYNAMIC DISASSEMBLY. THE SEQUENCE OF EVENTS POSTULATED FOR THE MODEL WAS AS FOLLOWS:
  - THE STORED STRAIN ENERGY IN THE CASING CAUSES THE CIRCUMFERENCE OF THE CASING TO CONTRACT RELATIVE TO THE CIRCUMFERENCE OF THE GRAIN. THIS INITIATES A DEBONDING ACTION.
  - THE INNER AND OUTER DIAMETERS OF THE GRAIN BEGIN TO EXPAND WHEN THE CASING IS CUT.
  - LARGE AMOUNTS OF THE GRAIN EXCEED THE FAILURE STRAIN RELATIVELY QUICKLY IN THE REGION 30^{o} ON EITHER SIDE OF THE LSC.
  - CRACKS DEVELOP IN THIS REGION OF HIGH STRAIN. THESE CRACKS MAY BE CONCEPTUALIZED AS POROSITY DISTRIBUTED OVER THE REGION OF HIGH STRAINS. THE ADJACENT VUGRAPH SHOWS HOW SUCH A PATTERN MIGHT DEVELOP.
  - GAS FLOWS THRU THIS POROSITY FROM THE CHAMBER TOWARD THE ATMOSPHERE.

EARLY-MET MODEL FORMULATION POSTULATING CASE SEPARATION, CAVITY DEVELOPMENT, GRAIN FRAGMENTATION AND CASING FRAGMENTATION

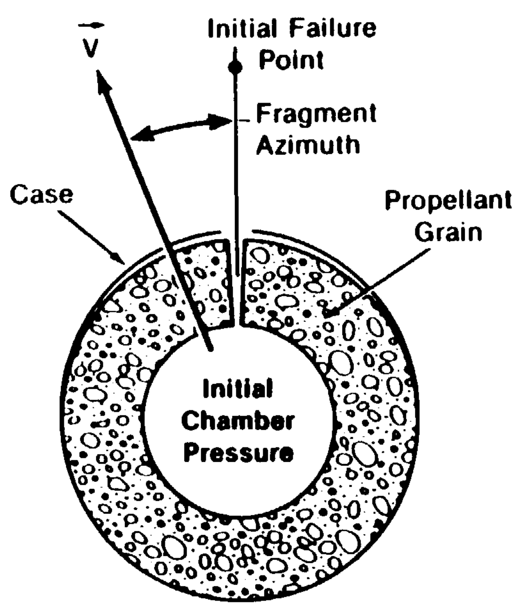

Release of Strain Energy Stored in Casing Causes a Shortening of Casing Circumference. High Tangential and Lower Radial Casing Velocity Relative to Grain Debonds Case from Grain. This Geometry Represents Zero Time for all Subsequent Calculations.

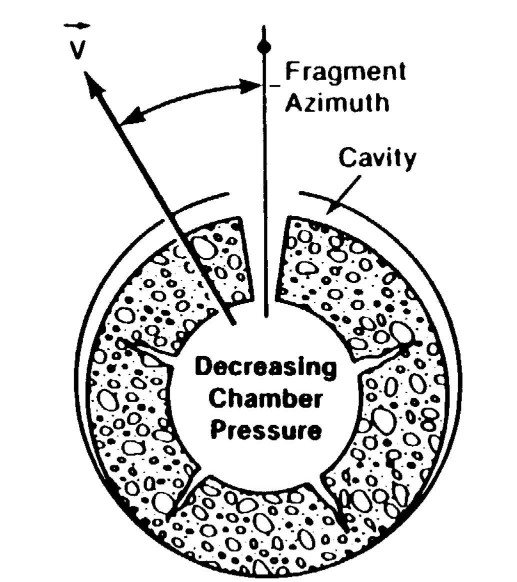

Cracks Initiate in Grain on Inner Diameter and Grain Begins to Fragment. Flow Passages Open Between Chamber and Cavity. Casing Begins to Accelerate Away from Grain.

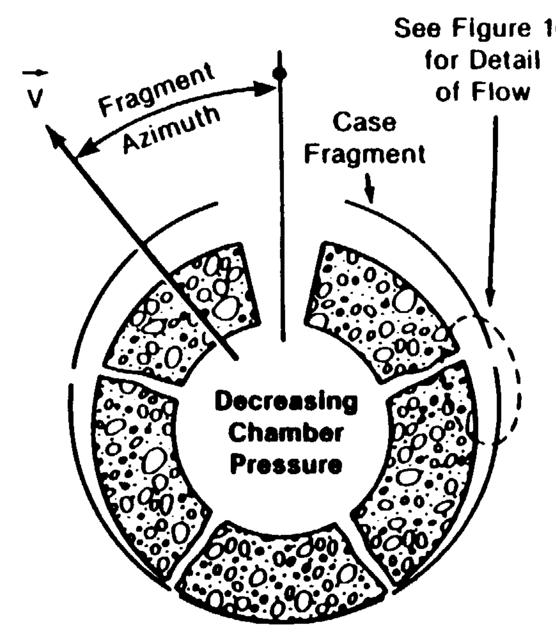

Casing Fragmentation Begins. Grain Acceleration Widens Flow Passages into Cavity. Casing Fragmenting Opens Flow Passages to Atmosphere.

S-087 10 07-88C

RELATIVE MOTION OF CASING AND GRAIN SHOWING CONNECTED VOIDS DEVELOPING IN HIGH STRAIN AREAS

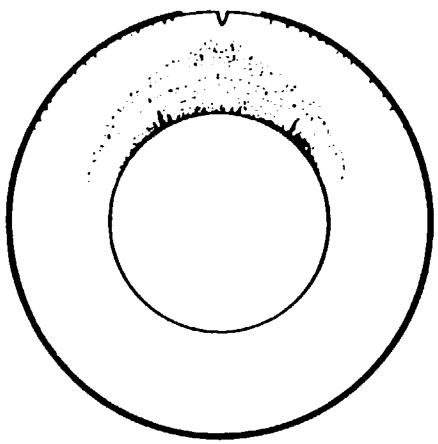

Shortly After LSC Initiation, Casing Debonds and Edge Retracts. Grain ID Begins to Grow and Areas of Plastic Strain Develop.

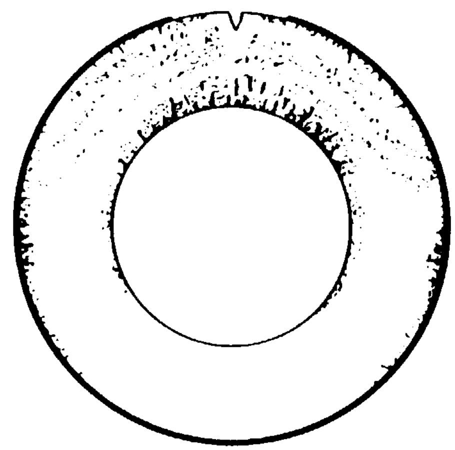

As Casing Retraction Continues, Chamber Bore Begins to Reach Failure Strain. Grain OD Grows and Areas of High Plastic Strain Propagate. Micro-Cracks Develop in High Strain Regions.

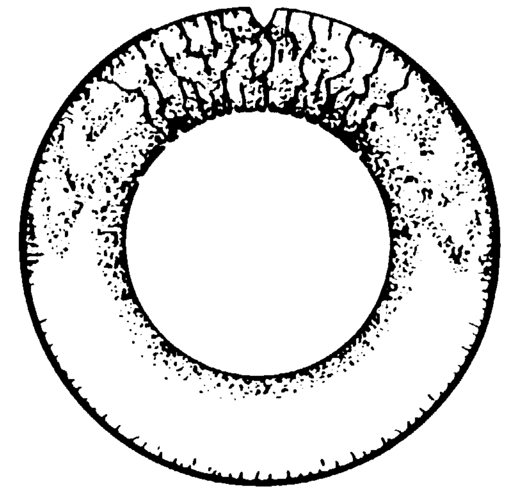

As Process Continues In Time, Micro Cracks Coalesce Into Connected Voids. These Voids Form Flow Channels Which Allow Venting of Chamber Gas to Atmosphere. Casing Blocks Flow and a Grain-Casing Cavity Forms. Casing Edge (Lip) Passes Over Crack. This Provides a Mechanism for Rapid Cavity Pressurization.

S-087.112R 02-89C

CAVITY PRESSURIZATION (CONT'D)

- THE LSC-CUT-EDGE OF THE CASING BLOCKS THE GAS FLOW TO THE ATMOSPHERE, CAUSING PRESSURIZATION OF THE VOLUME BETWEEN THE CASING AND THE GRAIN. (IF THERE IS NO VOLUME, THERE IS NO RELATIVE MOTION OF THE CASE AND GRAIN; THEREFORE, FRAGMENT VELOCITY WILL BE THE SAME AS IN THE BONDED CASE.)

- IN REALITY, THE CASING EDGE WILL PASS OVER A NUMBER OF SMALL FLOW CHANNELS WHICH HAVE BEEN FORMED BY CONNECTING THE POROSITY INTRODUCED INTO THE GRAIN AT LOCATIONS WHERE THE PBAN EXCEEDS ITS LOCAL STRAIN TO FAILURE.

- LUMPING THE DISTRIBUTED POROSITY IN THE PBAN FRACTURED ZONE INTO A SINGLE CHANNEL IS CONSERVATIVE BECAUSE IT NEGLECTS THE ASPECT RATIO LOSS CONSIDERATIONS IN THE SERIAL SUPERSONIC NOZZLES CREATED WITHIN THE FRACTURED ZONE.

- THE TOTAL FLOW AREA OUT OF THE CHAMBER AND THE CAVITY MUST BE DETERMINED BY SOLVING THE EQUATIONS OF MOTION, THE MATERIAL CONSTITUTIVE EQUATIONS AND THE GAS DYNAMICS EQUATIONS SIMULTANEOUSLY. ALL OF THE MATERIALS (CASING, GAS AND GRAIN) MUST BE INCLUDED IN THIS EVALUATION.

- FROM THE STANDPOINT OF THE EQUATIONS OF MOTION, IT DOES NOT MATTER THAT THE POROSITY IS LUMPED. ONLY SO MUCH FLOW AREA CAN OCCUR FROM GRAIN MOTION IN A GIVEN PERIOD OF TIME. (F = MA)

LATE MET MODELS

- THE PHYSICAL EVIDENCE OF THE 51L-EVENT IMPLIED THAT THERE IS A GRAIN THICKNESS AT WHICH DEBONDING WILL NOT OCCUR.

- IT WAS ESTIMATED BY OTHERS THAT THIS TRANSITION WOULD OCCUR AT APPROXIMATELY 105 SECONDS MET WHEN THE GRAIN WAS APPROXIMATELY SIX INCHES THICK.

- A LATE MET MODEL WAS DEVELOPED TO HANDLE THE SPECIAL CASE OF NO FUEL-CASING DEBONDING.

LATE MET MODELS (CONT'D)

- THE LATE MET MODEL IS A FULLY COUPLED EULERIAN-LAGRANGIAN MODEL WHICH SOLVES THE SRM MATERIAL CONSTITUTIVE EQUATIONS, THE EQUATIONS OF MOTION, AND THE GAS DYNAMICS EQUATIONS SIMULTANEOUSLY.
    - NO CAVITY IS FORMED IN THIS MODEL.
    - GRAIN AND CASING DO NOT DEBOND.
    - 2D MOTION OF GRAIN AND CASING ARE ASSUMED; HOWEVER, 3D-FLOW IS CONSIDERED FOR RANDOM FAILURE CASES.
    - SINCE THE AFT CYLINDER OF ONE OF THE SEGMENTS OF INTEREST HAD NO FUEL REMAINING AT 110 SECONDS MET, IT WAS NECESSARY TO RUN TWO CASES WITH THIS MODEL (2.7 INCHES OF GRAIN REMAINING AND NO GRAIN REMAINING.)
- THE LATE TIME RSD AND RANDOM FAILURE MODELS ARE SIMILAR. EXAMPLES OF THE MODEL AND ITS RESULTS WILL BE PRESENTED SUBSEQUENTLY.

RANDOM FAILURE MODELS

- THE RANDOM FAILURE EVENTS REQUIRED DETAILED MODELING OF THE LONGITUDINAL HOT GAS FLOW AS WELL AS OF THE RADIAL HOT GAS FLOW.
    - REDUCTION OF THE 34D-9 SRM-2 DATA SHOWED THAT THE OBSERVED FRAGMENT VELOCITIES HAD A PRONOUNCED LONGITUDINAL POSITION DEPENDENCE. THE TREND OF THIS DEPENDENCE IS SHOWN IN THE ADJACENT VUGRAPH.
    - THE SRM-2 FAILURE OCCURRED IN SEGMENT 1 AND A CRACK PROPAGATED UPWARD THRU SEGMENT 4. SEGMENTS 5 AND 6 DID NOT FRAGMENT, BUT FLEW AS A SINGLE COMPONENT TO IMPACT ON AN ADJACENT PAD.
    - THE NET EFFECT OF THIS INITIAL LONGITUDINAL POSITION DEPENDENCY DELAY IN FRAGMENTATION INITIATION WAS TO ALLOW THE CHAMBER PRESSURE TO FALL BELOW THE LEVEL REQUIRED TO FRAGMENT THE GRAIN AND CASING OF SEGMENTS 5 AND 6.

CORRELATION OF PREDICTED AND OBSERVED RESULTS FROM THE 34D-9 SRM RANDOM FAILURE

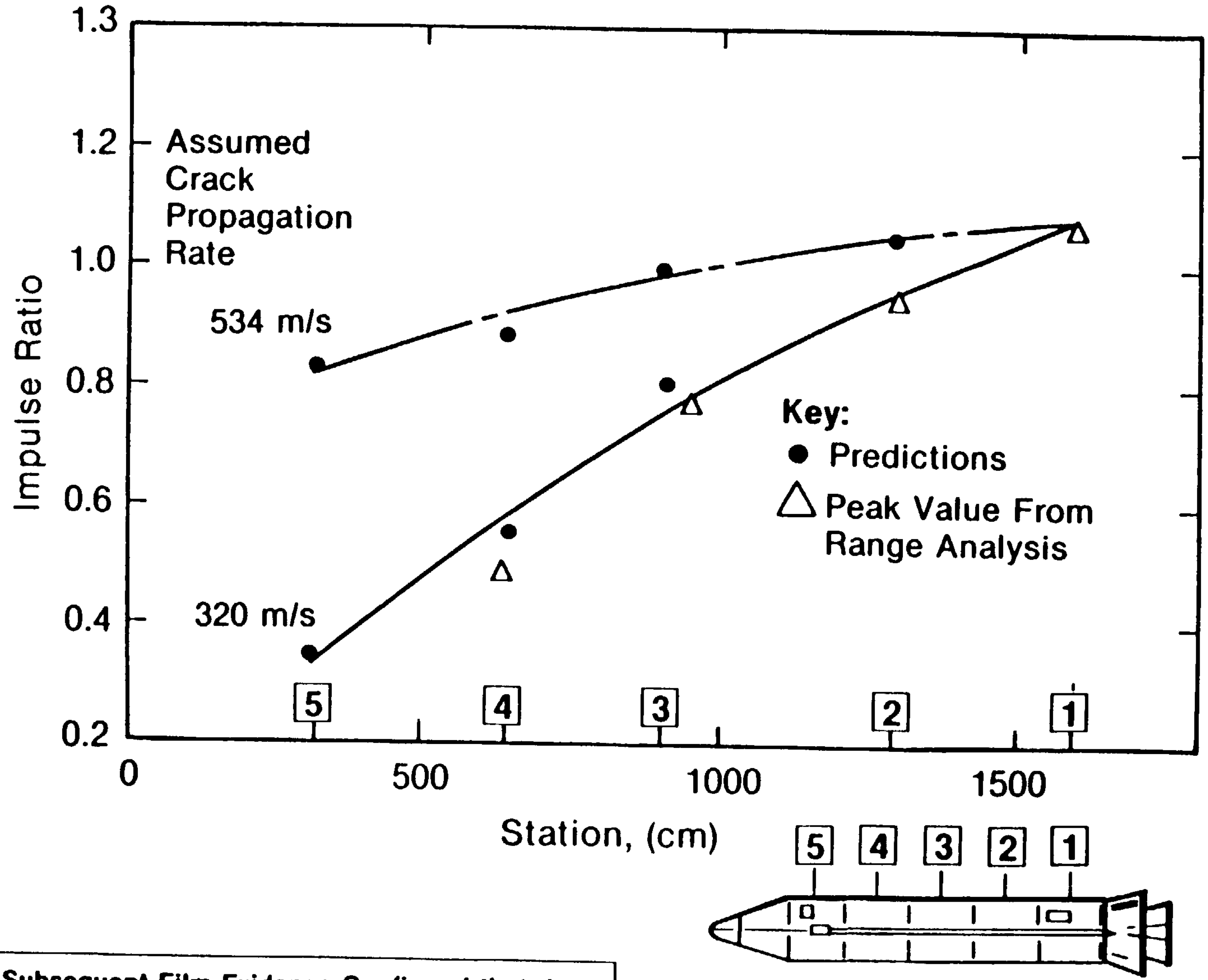

Note: Subsequent Film Evidence Confirmed that the Effective Crack Propagation Rate was 320 m/s

S-087.17 02-89C

RANDOM FAILURE MODELS (CONT'D)

- THE EFFECT OF LONGITUDINAL FLOW ON THE ENERGY STORED IN ANY SRM SEGMENT WAS ASSESSED AS A FUNCTION OF TIME WITH AN AXISYMMETRICAL FLOW MODEL WHICH ALLOWED SEGMENT LEAKAGE AREA TO VARY AS A FUNCTION OF TIME. THIS EFFECT IS SHOWN IN THE ADJACENT VUGRAPH.

- A FULLY COUPLED Z-FLOW MODEL WAS USED TO ASSESS THE FRAGMENT VELOCITIES GENERATED BY LATE MET RANDOM FAILURE. THE RESULTANT FLOW FIELD AND PREDICTED FRAGMENT VELOCITIES ARE SHOWN IN THE ADJACENT VUGRAPHS.

- IT WAS FOUND THAT THE FRAGMENT VELOCITIES RESULTING FROM RANDOM SRM CASING FAILURE WERE 0.30 TO 1.07 TIMES THOSE OF THE EQUIVALENT SEGMENT FRAGMENT VELOCITIES DEVELOPED IN RSD INITIATED EVENTS.

TIME-HISTORY OF THE PRESSURE AT FIVE LONGITUDINAL DISTANCES FROM THE 34D-SRM HEAD AFTER RANDOM FAILURE IN SEGMENT 1 AT 10 SECONDS MET FOR TWO CRACK PROPAGATION RATES

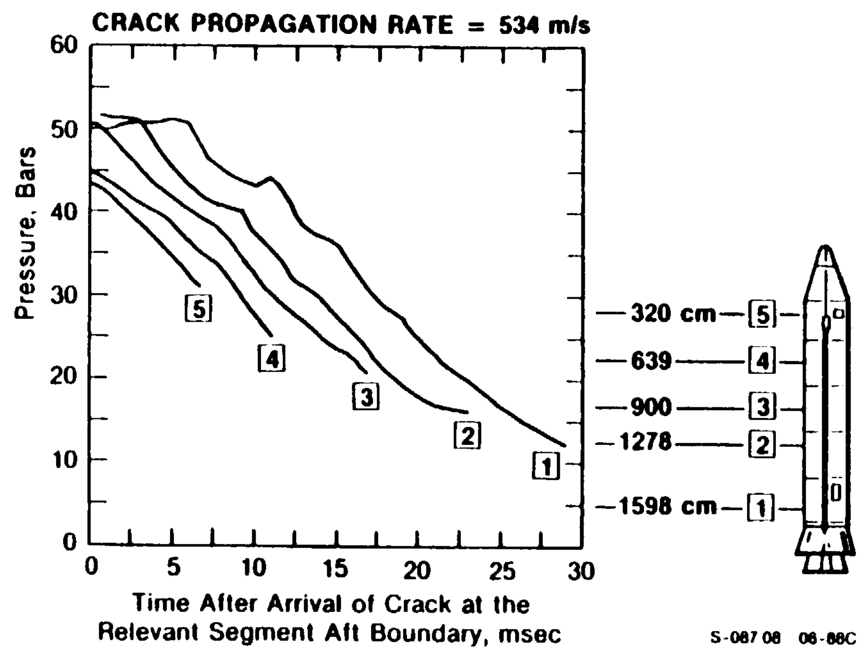

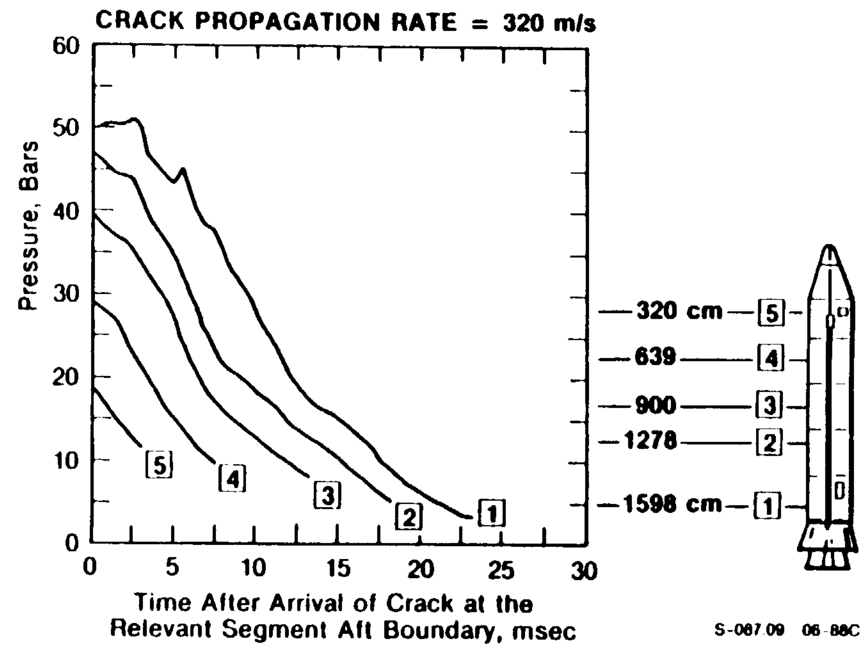

FLOW FIELD DEVELOPING AROUND A RANDOMLY FAILED STS CENTER-SEGMENT FORWARD-CYLINDER WITH FRAGMENTATION OCCURRING 5 msec AFTER INITIAL CASING FAILURE

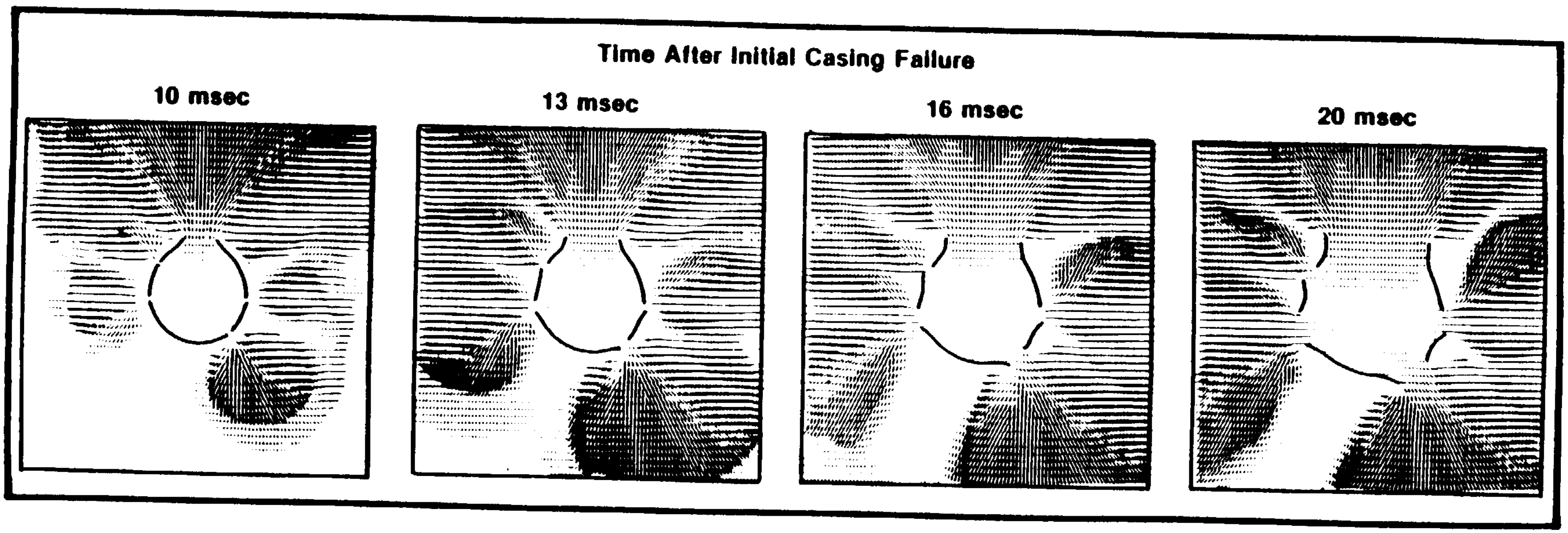

S-087.06 06-88C

STS-SRM CASING GEOMETRY FOR FOUR ASSUMED FRAGMENTATION TIMES 20 MSEC AFTER A RANDOM CASING FAILURE

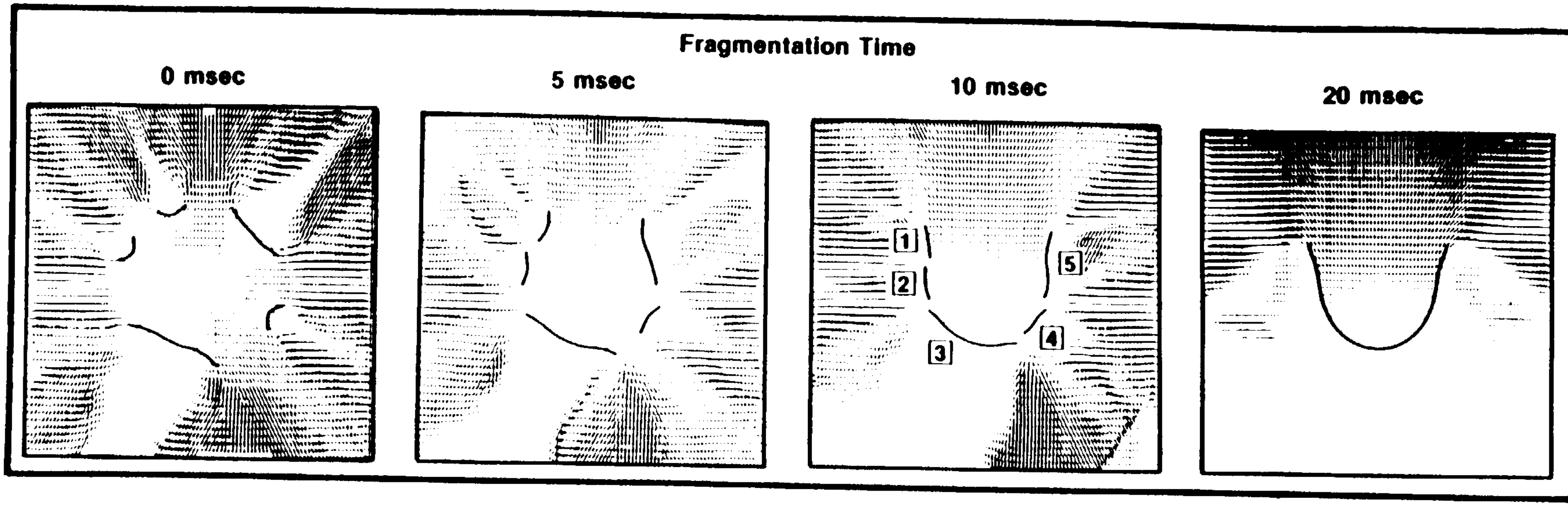

TIME-HISTORY OF FRAGMENT VELOCITIES RESULTING FROM THE RANDOM FAILURE OF A STS-SRM FOR FOUR ASSUMED FRAGMENTATION TIMES AT 110 SECONDS MET (SQUARED NUMBERS REFER TO FRAGMENTS SHOWN IN ABOVE FIGURE

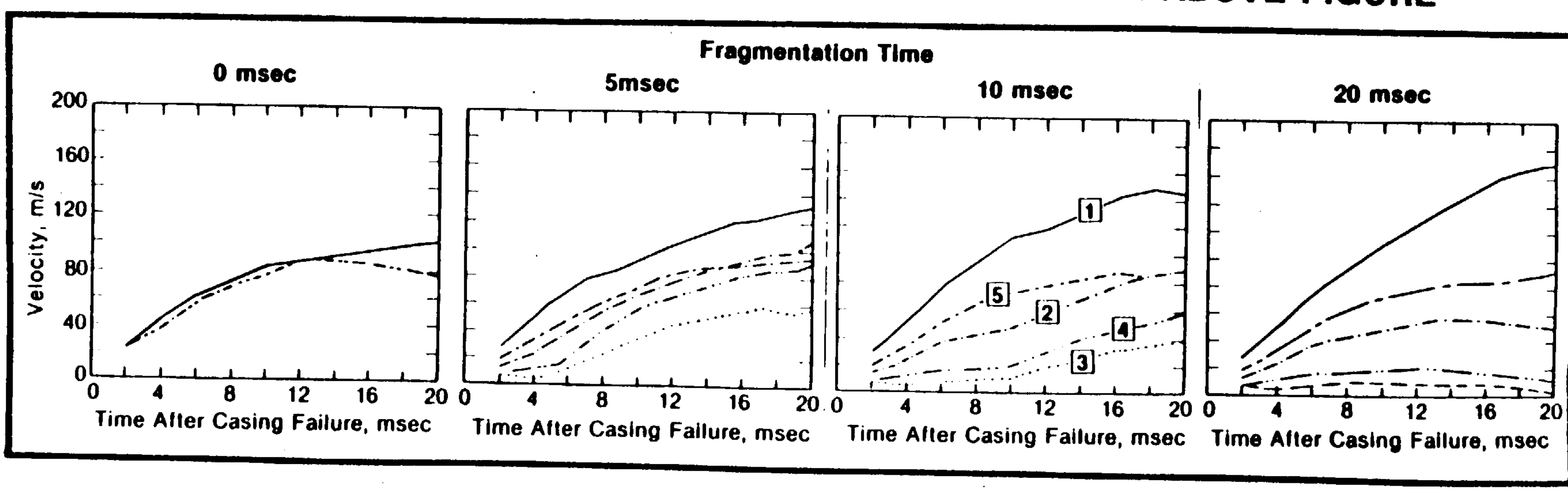

S-087.05 06-88C

POST-PROCESSOR MODEL

- THE POST-PROCESSOR MODEL WAS DEVELOPED TO PROVIDE A MEANS TO PERFORM THE SENSITIVITY STUDY NECESSARY TO UNDERSTAND THE OBSERVED 34D-9 FRAGMENT VELOCITY DISTRIBUTION.
    - JAFFE (JPL) NOTED THAT THE RESULTS FROM THE COUPLED EULER RUNS COULD BE NORMALIZED ACROSS BOOSTERS AND ACROSS MET. THIS ALLOWED A MECHANISM FOR PRODUCING A FAST RUNNING "POST PROCESSOR" (STRESS BOUNDARY) MODEL.
    - THE NORMALIZED CURVES USED AS A FORCING FUNCTION FOR THE POST PROCESSOR MODEL ARE SHOWN IN THE ADJACENT VUGRAPH.
    - THE RESULTS OBTAINED FROM THE POST PROCESSOR MODEL WERE COMPARED TO THE 34D-9 DATA BASE AT 10 SECONDS MET.
    - NO VELOCITY IN THE DATA BASE EXCEEDED THAT PREDICTED BY THE COUPLED EULER-LAGRANGIAN CALCULATIONS-130 M/S FOR A FRAGMENT WITH PIECE 1564 GEOMETRY AND SRM FRAGMENTATION TIMES OF 5 TO 12 MSEC AFTER INITIAL GAS FLOW THRU THE GRAIN.

DIMENSIONLESS CHAMBER AND CAVITY PRESSURES AS A FUNCTION OF TIME AFTER LINEAR SHAPED CHARGE INITIATION

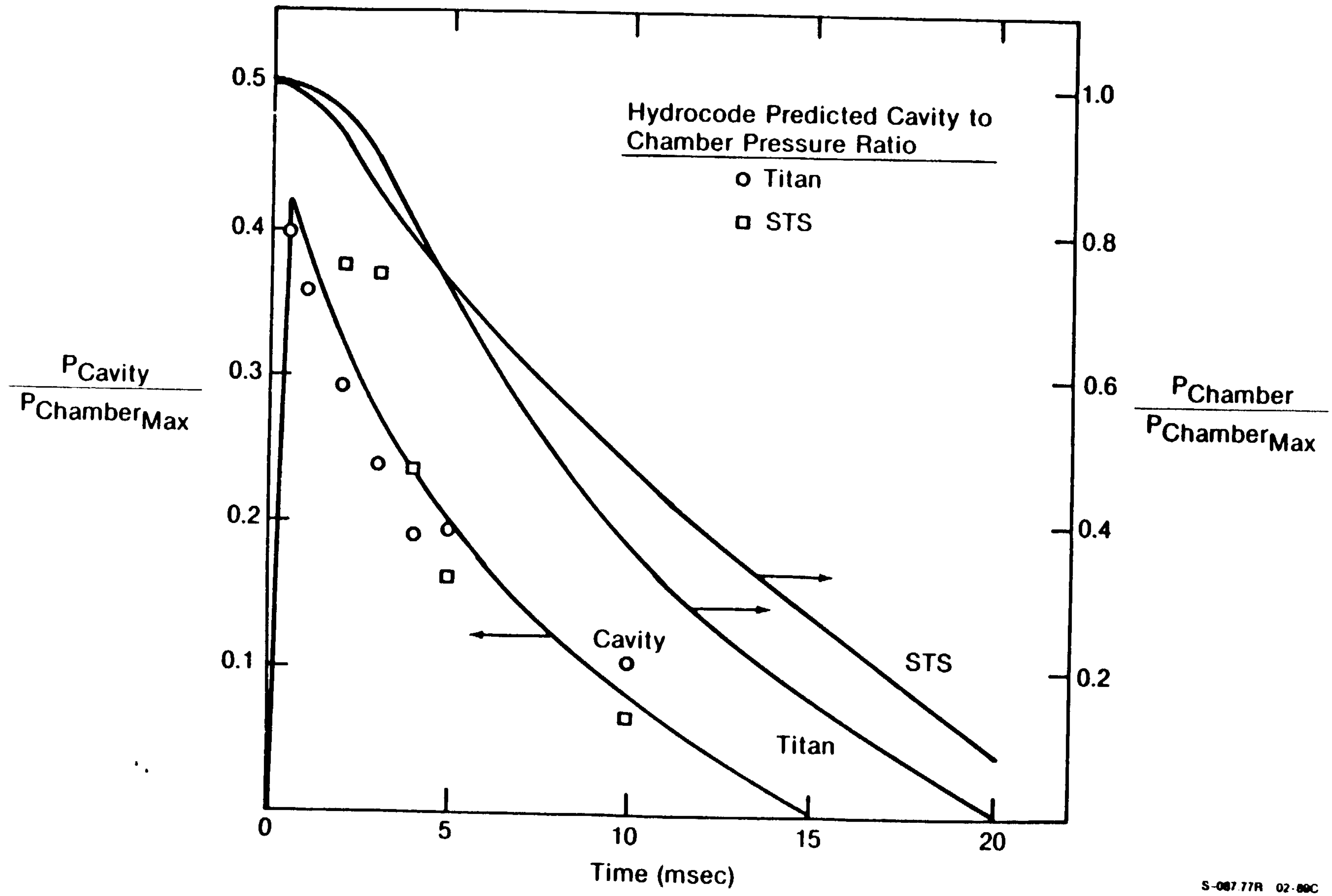

S-087.77R 02-89C

POST-PROCESSOR MODEL (CONT'D)

- A NUMBER OF FRAGMENTS HAD LOWER VELOCITIES THAN THOSE PREDICTED FOR THE FAST, CUTLINE FRAGMENTS.

- A FACTOR (K_p) WAS INTRODUCED TO ACCOUNT FOR THE DISTRIBUTION OF FRAGMENT VELOCITIES SEEN IN THE 34D-9 EVENT.

- THIS FACTOR WAS ALWAYS LESS THAN 1.0; i.e., K_p ALWAYS HAD THE EFFECT OF REDUCING THE PREDICTED VELOCITY TO PROVIDE FOR THE OBSERVED VELOCITY DISTRIBUTION.

- A SERIES OF 250 RUNS WAS MADE TO PROVIDE A STATISTICAL BASIS FOR THE FRAGMENT VELOCITY AND AZIMUTH ENVIRONMENT CREATED BY A VARIETY OF RANGE DESTRUCT AND RANDOM STS-SRM FAILURES OCCURRING BETWEEN 0 TO 110 SECONDS MET.

- THE ONLY VARIABLES IN THIS SERIES WERE THE CAVITY PRESSURE REDUCTION FACTOR (K_p) AND THE SRM CASING FRAGMENTATION TIME. (TIME OF FIRST GAS VENTING THRU THE GRAIN IS TIME ZERO.) TYPICAL RESULTS ARE PRESENTED IN THE ADJACENT VUGRAPHS.

34D-SRM CASING GEOMETRY FOR FOUR ASSUMED FRAGMENTATION TIMES 20 MSEC AFTER A RANGE DESTRUCT ACTION AT 10 SECONDS MET

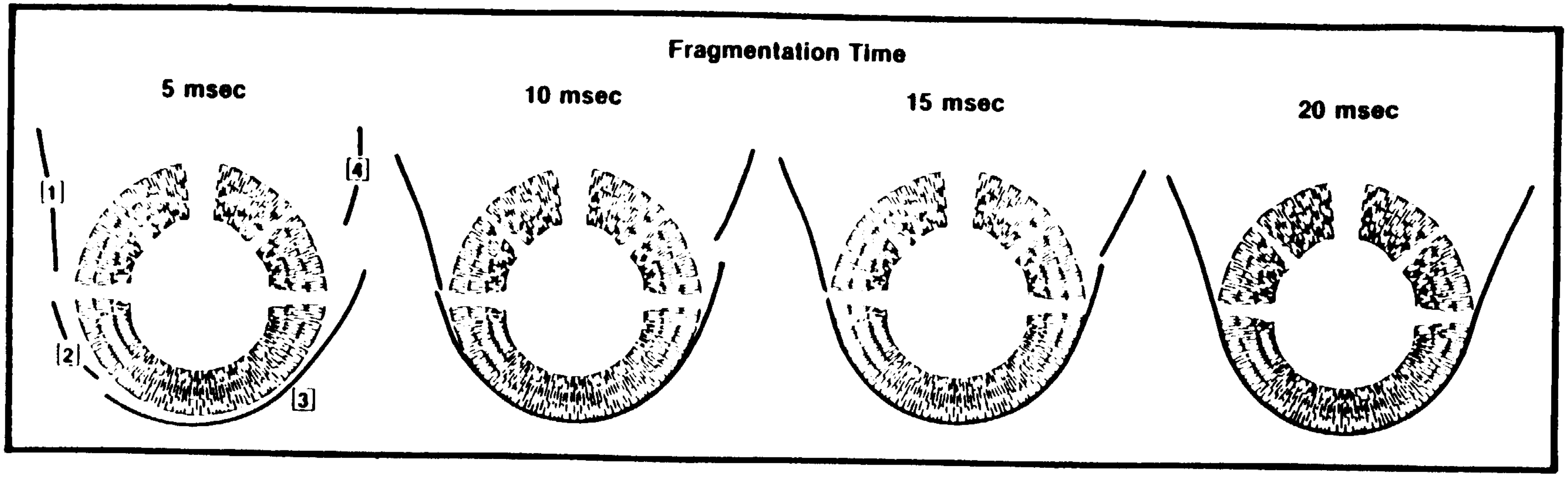

TIME-HISTORY OF FRAGMENT VELOCITIES RESULTING FROM THE RANGE DESTRUCTION OF A 34D-SRM FOR FOUR ASSUMED FRAGMENTATION TIMES AT 10 SECONDS MET (SQUARED NUMBERS REFER TO FRAGMENTS SHOWN IN ABOVE PANEL)

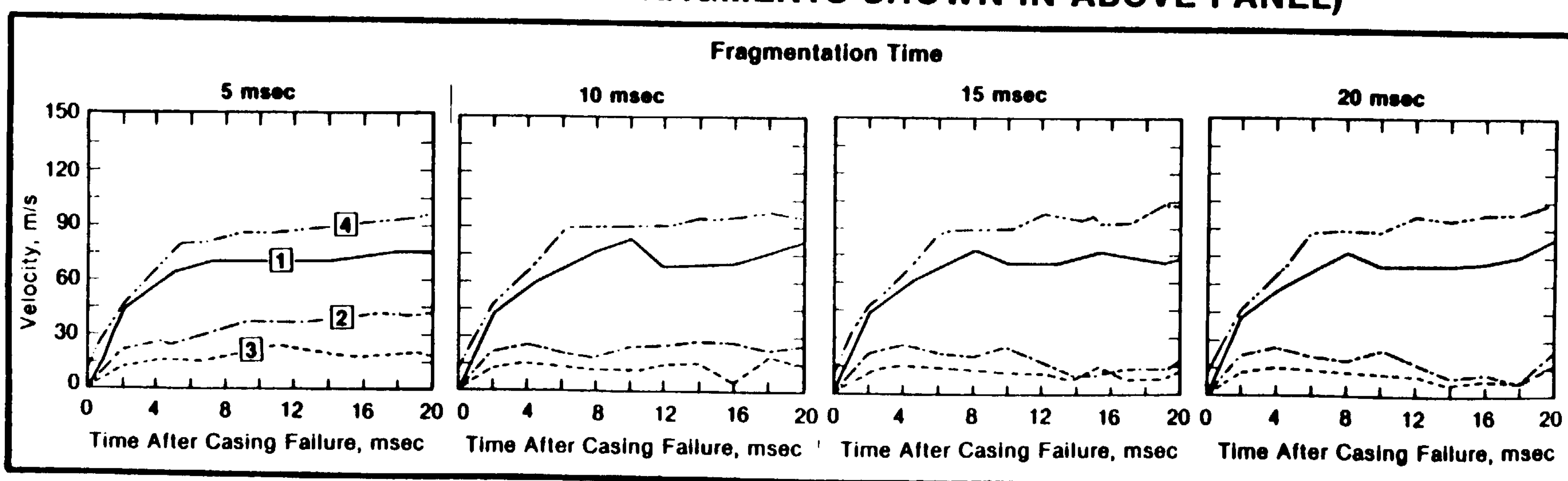

EFFECT OF FRAGMENTATION TIME ON THE VELOCITY AND AZIMUTH OF THE HIGHEST VELOCITY 34D-SRM FRAGMENTS (Number 4, FAST OCTANTS), SHOWN IN ADJACENT VUGRAPH

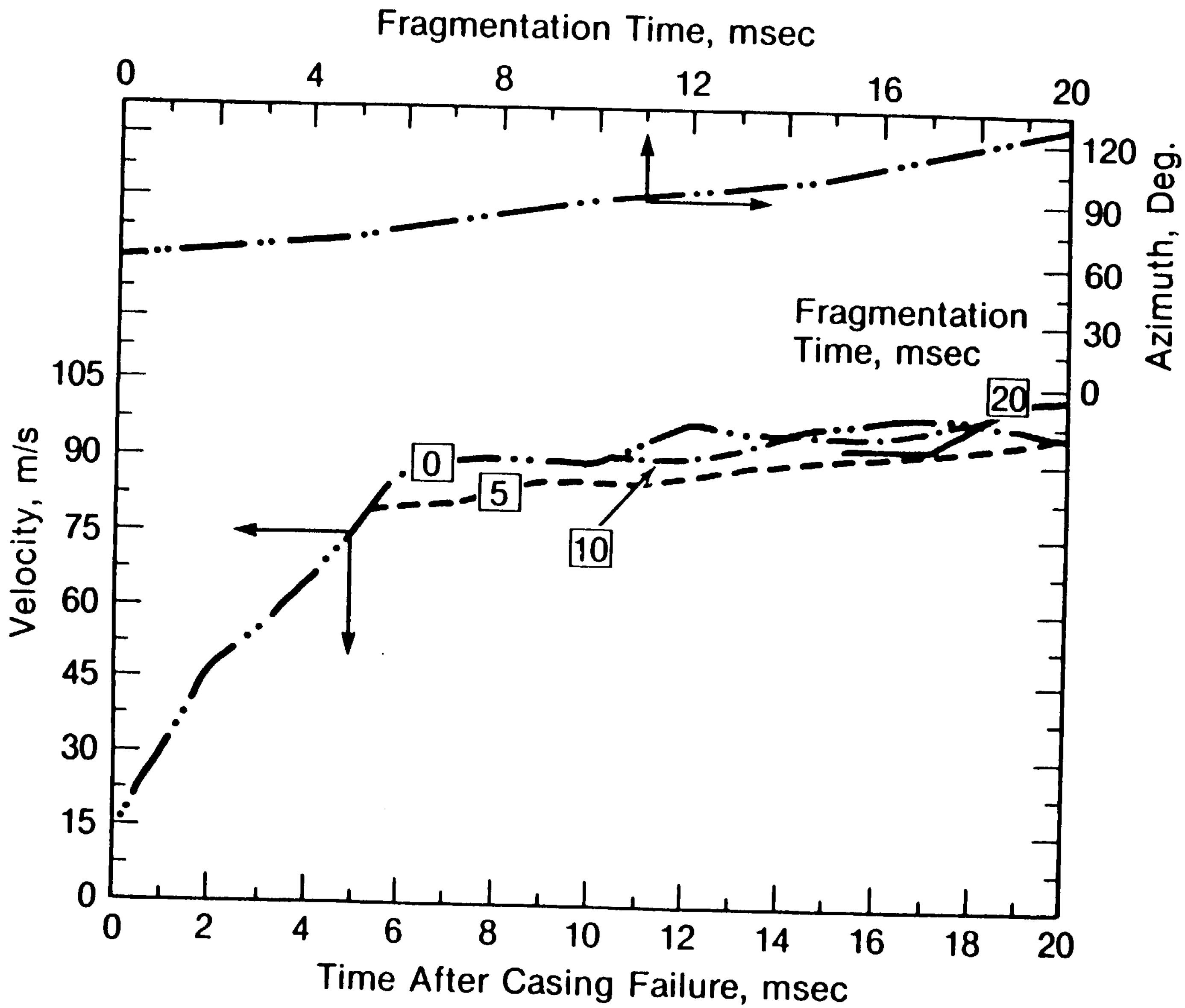

S 087 13 06-88C

POST PROCESSOR MODEL (CONT'D)

- POST PROCESSOR MODEL RUNS DID NOT COUPLE THE GAS DYNAMICS TO THE MOVEMENT OF THE SRM MATERIALS.

- THE NORMALIZED PRESSURE-TIME-HISTORY WAS APPLIED TO THE RELEVANT AREAS OF THE VARIOUS COMPONENTS AS A STRESS BOUNDARY AND THE EQUATIONS FOR MOTION WERE SOLVED IN LAGRANGIAN COORDINATES.

- CRITICISMS OF THE MANNER IN WHICH THE VARIOUS SRM MASSES WERE ALLOWED FREEDOM TO MOVE (INDUCED SLIDE LINES) HAVE BEEN MADE.

- THESE CRITICISMS ARE BASED ON THE NOTION THAT MATERIAL STRENGTH PLAYS A LARGER ROLE THAN MATERIAL INERTIA IN EVENTS WHICH OCCUR IN A 20 TO 30 MSEC TIME FRAME.

- THE RELATIVE IMPORTANCE OF THESE FACTORS WILL BE DISCUSSED SUBSEQUENTLY.

MODEL DEVELOPMENT CONCLUSION

- THE UTILITY OF THE MODEL IS BEST DETERMINED BY ASSESSING HOW WELL ITS PREDICTIONS MET THE PROGRAM OBJECTIVES.

  THIS ASSESSMENT WAS MADE BY COMPARING THE MODEL PREDICTIONS TO THE RESULTS OBSERVED FOR THE 34D-9 AND STS-51L EVENTS.

  AS CAN BE SEEN FROM THE ADJACENT VUGRAPHS, GOOD AGREEMENT BETWEEN PREDICTIONS AND OBSERVATIONS WAS OBTAINED FOR FRAGMENT:

  - VELOCITY
  - VELOCITY DISTRIBUTIONS
  - AZIMUTHS
  - ROTATION RATES

- BASED ON THIS AGREEMENT WITH THE ENTIRE DATA BASE, THE MODEL WAS USED TO PREDICT THE PROBABLE FRAGMENT ENVIRONMENTS WHICH WOULD OCCUR IN THE EVENT OF STS-SRM RSD OR RANDOM FAILURE AT 10, 74, 84, AND 110 SECONDS MET.

- THE RESULTS OF THESE PREDICTIONS ARE THE BASIS OF THE FRAGMENT ENVIRONMENTS PRESENTED IN THE SHUTTLE DATA BOOK (NSTS-08116).

COMPARISON OF THE OBSERVED AND PREDICTED FRAGMENT VELOCITY AND AZIMUTH RESULTING FROM THE RANGE DESTRUCT OF SRM-1 IN THE 34D-9 EVENT

	Observations Based On T34D-9 Range Data					Predictions Based On Hydrocode Calculations					
	Segment	Piece	Range (m)	Azimuth* (deg)	Velocity (m/s)	AZ* (deg)	FT† (ms)	VEL (m/s)	AZ* (deg)	FT† (ms)	VEL (m/s)
						Kp** = 0.8			Kp** = 1.0		
	1	497	418	108	105	107	18	89	107	18	105
	3	493	362	115	105	110	18	91	110	18	106
	3	500	350	84	99	86	10	84	85	10	102
	4	427	346	76	88	86	10	82	86	10	99
	5	1564	356	−58	100	−78	8	98	−76	8	119
						Kp** = 0.2			Kp** = 0.4		
	1	520	248	−86	56	−86	12	38	−86	12	59
		538	194	−56	39	−91	10	27	−91	10	41
	2	480	162	71	30	91	10	27	91	10	41
	4	484	251	128	53	109	18	45	109	18	59
		1077	133	−63	27	−91	10	29	−91	10	45
	5/6	483	206	117	43	106	18	22	106	18	64

*Initial Casing Failure at 0 Degree

**Arbitrary Cavity-Pressure Reduction Factor Used to Match Observed Results[7]

†Fragmentation Time.

S-087.25 06-88C

COMPARISON OF PREDICTED AND MEASURED VELOCITIES FOR AN STS-SRM AT 110 SEC MET

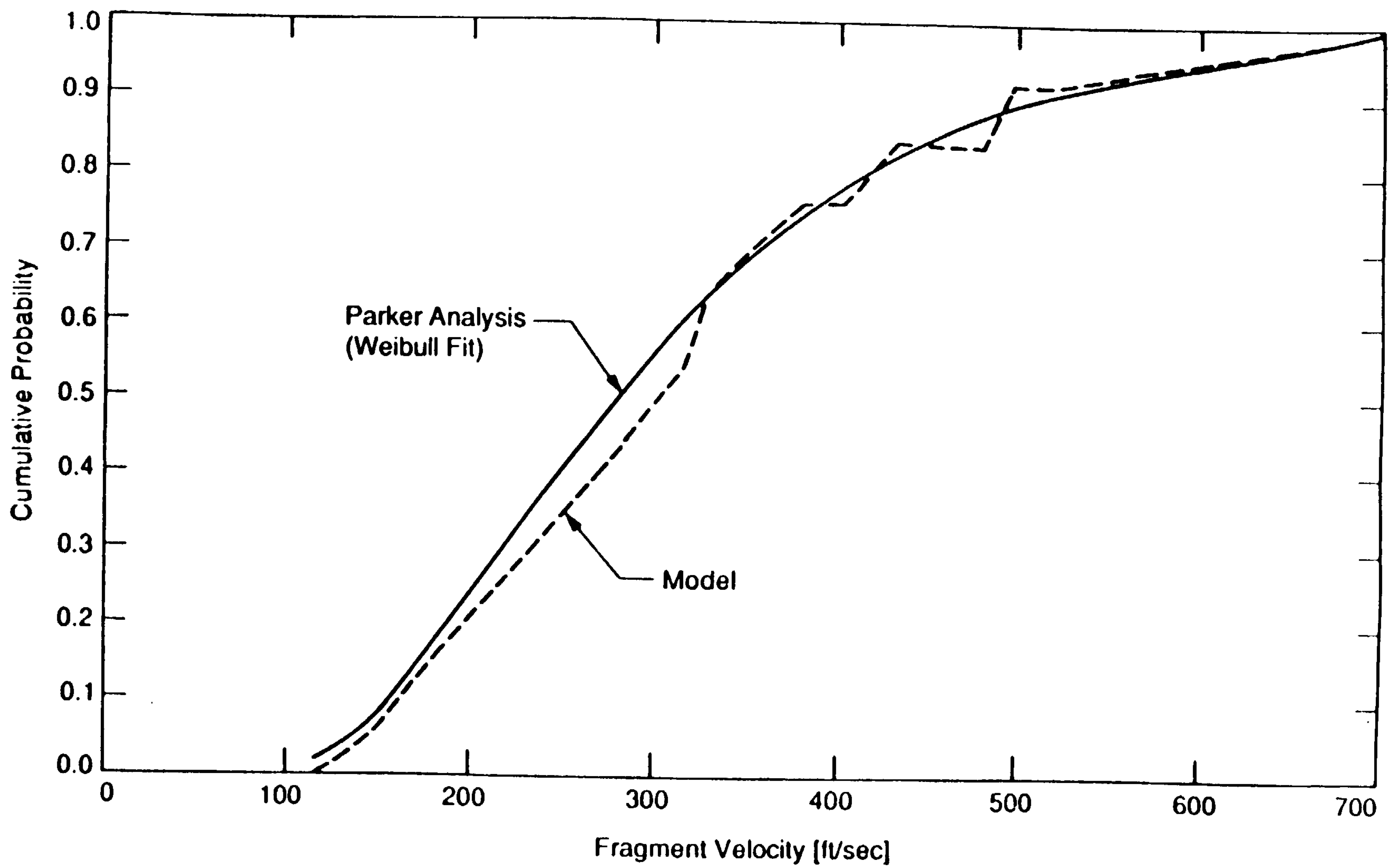

SUMMARY OF THE PREDICTED AND OBSERVED FRAGMENTATION RESPONSE OF SEVERAL VEHICLE ELEMENTS TO A NUMBER OF INTERNAL PRESSURE ENVIRONMENTS

Booster / Event	Vessel Pressure at Time of Initial Failure	Failure MET	Fragmentation Time[a]	Predicted Range of Fragment Velocities[e] [f]	Observed Range of Fragment Velocities	Predicted Range of Fragment Rotation Rates[e]	Observed Range of Fragment Rotation Rates
	Bar	sec	msec	m/s	m/s	Hz	Hz
34D-9 Range Destruct	54.5	10.	0-20	17-104	15-106[c]	8-12	5-12
34D-9 Random[b] Failure	54.5	10.	0-20[d]	15-111	15-114[c]	8-12	5-12
STS Range Destruct	60.	10	0-20	2-108	—	1-12	—
STS Random Failure	60.	10	0-20	2-115	—	1-12	—
STS Range Destruct	41.4	84.	0-20	30-104	—	1-11	—
STS Random Failure	41.4	84.	0-20	53-123	—	1-12	—
STS-51L Range Destruct (Fwd. Cyl.)	31.0	110.	0-20	6-162	15-198	0-11	3-17
STS-51L Range Destruct (Aft. Cyl)	31.0	110.	0-20	19.8-226.	15-198	1-19	3-17
STS Random Failure (Fwd. Cyl.)	31.	110.	0-20	3.-169.	—	0-12	—

[a] Time after initial grain fragmentation at which casing fragments are generated. The latest time at which shell stresses can be supported by casing-materials' strength.

[b] A 320 m/s propagation rate is used to communicate the crack from segment to segment.

[c] Based on analyses of range data performed by Jaffe[3] using a six degree of freedom code.

[d] Instantaneous fragmentation is assumed in the randomly failed segment followed by subsequent segment casing failure up to 20 msec after the arrival of a propagating (320 m/s) crack at the relevant segment boundary.

[e] Ranges vary from early-fragmentation-large-fragments to late-fragmentation time-small fragments adjacent to the initial casing-crack free-surface.

[f] Note that all random failure generated fragment velocity ranges are for the fragmented cylinder. The cylinders adjacent to this cylinder will have serially decreasing maximum fragment velocities. This decrease may be more than a factor of two when the randomly failed cylinder is at a stack extreme. At low crack propagation rates the extreme cylinder may not fragment.

MODEL REVIEW AND BOUNDARY ASSUMPTION VERIFICATIONS

- SANITY CHECKS -

- IT IS ALWAYS USEFUL TO STEP BACK AND ASK IF WHAT IS BEING MODELED MAKES PHYSICAL SENSE.

- SEVERAL INVESTIGATORS HAVE SUGGESTED THAT THE TOTAL ENERGY STORED IN THE STS-SRM AT 10 SECONDS MET IS SIGNIFICANTLY HIGHER THAN THAT STORED IN THE 34D-SRM. THIS ARGUMENT IS VALID; HOWEVER, AS SHOWN IN THE ADJACENT VUGRAPH, IT MISSES THE POINT.

- THE PISCES CODE IS WELL KNOWN AND WELL CALIBRATED. THIS NOT-WITHSTANDING, HYDROCODE MODELING HAS A NUMBER OF PITFALLS AND IT IS RELATIVELY EASY TO GET TRAPPED IN THEM.

- STEVE HANCOCK, THE PRINCIPAL AUTHOR OF THE PISCES CODE, WAS RETAINED TO REVIEW THE PREVIOUSLY PRESENTED WORK.

- MR. HANCOCK PERFORMED A NUMBER OF ANALYSES TO PROVIDE FIRST ORDER PREDICTIONS OF THE RELATIVE MOTIONS OF SRM CASING AND GRAIN FRAGMENTS ASSUMING RADIAL TRAJECTORIES FOR BOTH. THE ANALYTICAL MODELS USED TO GENERATE THESE RESULTS ARE SHOWN IN THE ADJACENT VUGRAPHS.

- THE PURPOSE OF THESE ANALYSES WAS TO BOUND THE RANGE OF VELOCITIES WHICH COULD BE PRODUCED BY THE AVAILABLE ENERGY AND THE PROBABLE PARTITION OF THAT ENERGY.

TITAN 34D AND STS[1] SIMILITUDE

- TITAN AND STS CHAMBER GAS ENERGY RATIO PER UNIT LENGTH AT 10 SEC MET

$$\frac{(PV)_{34D}}{(PV)_{STS}} \equiv \left(\frac{\text{Chamber Pressure}_{34D}}{\text{Chamber Pressure}_{STS}}\right)\left(\frac{(\text{Average Chamber Diameter}_{34D})^2}{(\text{Average Chamber Diameter}_{STS})^2}\right)$$

$$\frac{(PV)_{34D}}{(PV)_{STS}} = \left(\frac{793}{843}\right)\left(\frac{(53.4)^2}{(65.6)^2}\right) = 0.62$$

- TITAN AND STS CASING, JOINT AND INSULATION MASS RATIO PER UNIT LENGTH

$$\frac{\text{Mass}_{34D}}{\text{Mass}_{STS}} = \left(\frac{576}{900}\right) = 0.64$$

- FIRST ORDER SIMILITUDE EXPECTATION

$$\frac{\text{Velocity}_{34D}}{\text{Velocity}_{STS}} = \left(\frac{\text{Chamber Energy Ratio}}{\text{Mass Ratio}}\right)^{1/2} = \left(\frac{0.62}{0.64}\right)^{1/2} = 0.98$$

CONCLUSION:

One Would Expect the Observed 34D-9 SRM-1 Fragment Environment to be a Good Approximation of an STS Fragment Environment Generated by an RSD at ~10 Seconds MET

1) STS Parameters from NSWC TR 80-417 (Reference Memorandum J. A. Roach to J. Petes)

S-087.116R 02-89C

SUMMARY OF UNIT STORED ENERGY AND UNIT MASS FOR THE 34D AND STS SRM AT VARIOUS MET

SRM Type	MET sec	PBAN Grain Mass kg/ft	Casing + Joint + ½ Insulation Mass kg/ft	Stored Energy eu(1)/ft	Ratio of Stored Energy to Grain Mass eu/kg	Ratio of Stored Energy to Casing Mass eu/kg	Ratio of Stored Energy to the Sum of Casing and Grain Mass eu/kg
34D	10	3131.	261.	182.	.0581	.697	.0536
STS	10	4636.	408.	281.	.0606	.689	.0557
STS	37	3745.	408.	406.	.109	1.00	.0978
STS	84	1905.	408.	650.	.214	1.59	.281
STS-FWD-CYL	110	426.	408.	663.	1.56	1.62	.794
STS-STAR-GR	110	0.0	539.	721.	-	1.34	1.34
STS-STAR-GR	20	0.0	539.	1408.	-	2.61	2.61

(1) One eu = 10^{12} ergs.

CONCLUSIONS:

1. The Ratio of Unit Stored Energy to Unit Casing Mass is Greater in a 34D-SRM than it is in an STS-SRM
2. This is Consistent with the Shuttle Data Book Model Prediction that Fragments Generated by an RSD at 10 SEC MET will be Lower in Velocity for an STS-SRM then for a 34D-SRM.

S-087 100R 02 89C

MODEL REVIEW AND BOUNDARY ASSUMPTION VERIFICATIONS (CONT'D)

- SANITY CHECKS (CONT'D) -

- IN ADDITION, MR. HANCOCK WAS ASKED TO REVIEW THE MODELING ASSUMPTIONS TO MAKE SURE HIS CODE HAD NOT BEEN MISUSED.

  AMONG THE PHENOMENA MR. HANCOCK EVALUATED WERE:

  - THE EXTENT TO WHICH THE PROBLEM IS TWO-DIMENSIONAL (EFFECTS OF BENDING WAVE SPEED).

  - EFFECTS OF THE PRESENCE OF GRAIN ON GAS DYNAMICS. THESE EFFECTS ARE SHOWN ON THE ADJACENT VUGRAPH.

  - EFFECT OF FRAGMENT ROTATION ON GRAIN-CASING CAVITY PRESSURE. THIS EFFECT IS SHOWN ON THE ADJACENT VUGRAPH.

  - EFFECT OF 3D FLOW ON PRESSURE BETWEEN THE GRAIN AND THE CASING. THIS EFFECT IS ILLUSTRATED AND THE RESULTS ARE SHOWN ON THE ADJACENT VUGRAPHS.

- THE RESULTS OF THIS STUDY ARE SUMMARIZED AND COMPARED TO THE HYDROCODE MODEL PREDICTIONS. THESE RESULTS ARE SHOWN ON THE ADJACENT VUGRAPHS.

MASS AND ENERGY FLOW

Model Geometry

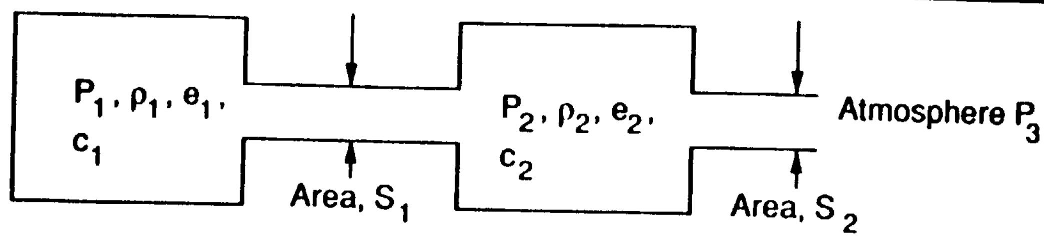

Mass Flow from Chamber i to Chamber i + 1 (i = 1 or 2)

$$\dot{M}_i = (C_{di}\, S_i + \Delta S_i)\, \rho_i\, c_i \sqrt{\frac{2}{\gamma - 1}\left(r_i^{\frac{2}{\gamma}} - r_i^{\frac{\gamma+1}{\gamma}}\right)}$$

{Discharge Coefficient} {Geometric Flow Area} {Optional Additional Area (Bypass)}

$$r_i = \max\left(\frac{P_{i+1}}{P_i},\ \left(\frac{2}{\gamma+1}\right)^{\frac{\gamma}{\gamma-1}}\right) = \text{Pressure Ratio}$$

Subsonic, Unchoked Flow — Choked Flow Limit

Energy Flow Rate from Chamber I to Chamber I + 1

$$\dot{E} = h_i \dot{M}_i$$

Where:

$$h_i = e_i + \frac{P_i}{\rho_i} = \text{Specific Enthalpy}$$

S-087.78W 2-89M

FRAGMENT EQUATION OF MOTION

$$M \frac{dv}{dt} = F$$

$$F = P_i\ (2h_i) - P_o\ (2h_o) + P_s\ (2h_o - 2h_i)$$

Where:

h = Half-Chord Lengths

P_s = Side Pressure (= P_i in Model at Present)

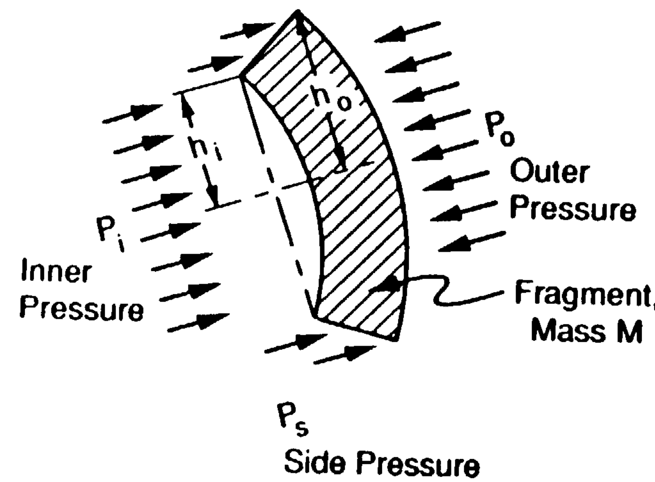

MASS AND ENERGY BALANCE FOR CHAMBER i

$P_i = (\gamma-1)\dfrac{E_i}{V_i}$ = Pressure

E_i = Total Internal Energy in Chamber i

V_i = Total Gas Volume in Chamber i

$c_i = \sqrt{\dfrac{\gamma P_i}{\rho_i}}$ = Sound Speed

$\rho_i = \dfrac{M_i}{V_i}$ = Density

M_i = Total Gas Mass

$\dfrac{dE_i}{dt}$ = − {Work Done on Fragments} − {Energy Flow to Next Chamber} + {Energy Flow from Chamber i-1 (If Any)}

$\dfrac{dM_i}{dt}$ = − {Mass Flow to Next Chamber} + {Mass Flow from Chamber i-1}

S-087.80W 2-89M

RIGID BODY 34D-9 MODEL RESULTS USED TO CHECK HYDROCODE RESULTS[1]

(Pressure = ATMOS., VELOCITY = m/s)

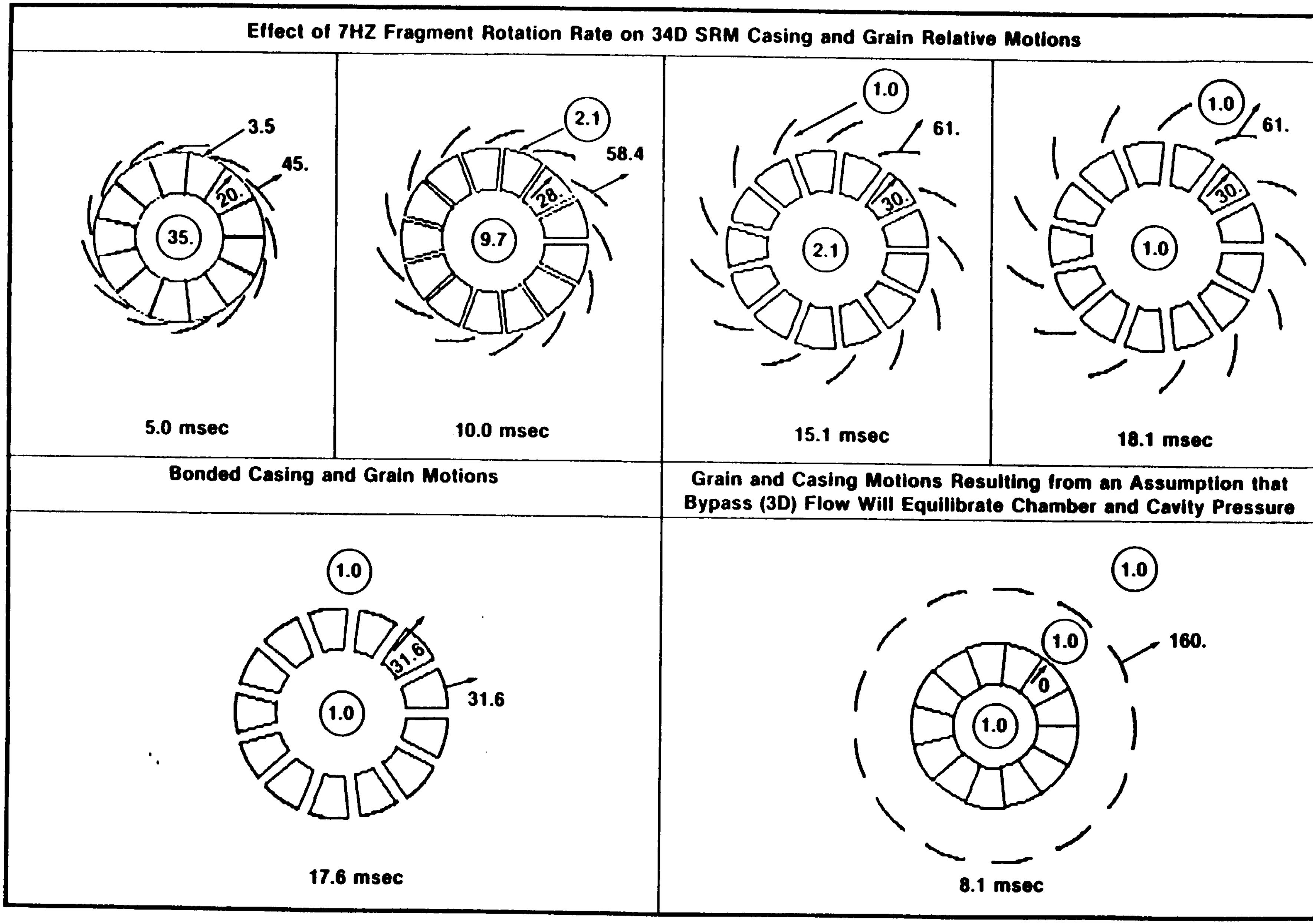

(1) Circled Numbers Are Pressures in Atmospheres; Numbers with Vectors Are Velocities in m/s

S-097.82R 02-89C

COMPARISON OF TWO-CHAMBER ANALYTICAL MODEL FRAGMENT VELOCITY FOR THE 34D AND STS-SRM AT MET = 10

SRM Type	E(1) Avail. Energy J/m	Mp PBAN Mass kg/m	Mc Case Mass kg/m	$\left(\frac{2E}{Mp + Mc}\right)^{1/2}$ m/s	$\left(\frac{2E}{Mc}\right)^{1/2}$ m/s	Vc Model 0 Hz m/s	Vc Model 7 Hz m/s
34D	1.83E7	10.3E3	724	58	224	78	56
STS	3.19E7	14.3E3	1112	64	239	83	54

(1) Available Energy = Work by Chamber Gas for an Isentropic Expansion to Atmospheric Pressure.

CONCLUSION:

The Predicted Ratio of Fragment Velocities is Consisitent With the First Order Similitude Expectation

S-087 99R 02-89C

PARAMETERS USED IN TWO-CHAMBER ANALYTICAL MODEL FOR THE 34D AND STS-SRM AT MET = 10

SRM Type	P_o Initial Chamber Pressure Pa	R_b Burn Radius (Vol. Avg.) m	R_c Case Radius m	H_c Case Thickness mm	V_o Chamber Volume m 3/m	f
34D	54.7E5	.678	1.528	9.5	1.44	.308
STS	58.6E5	0.864	1.83	12.2	2.35	0.314

Common Properties:

Gas Ratio of Specific Heats, γ =	1.142	
PBAN Density	1750	kg/m^3
Case Density	7860	kg/m^3

Available Energy $E = f P_o V_o / (\gamma - 1)$

Where:

$$f = 1 - r^{\left(\frac{\gamma-1}{\gamma}\right)} + (\gamma - 1)\, r\, (1 - r^{-\frac{1}{\gamma}})$$

$$r = P_a / P_o$$

S-087 101R 02-89C

TYPICAL SRM CYLINDER GEOMETRY SHOWING 34D AND STS JOINT DETAILS

34D Joint Detail

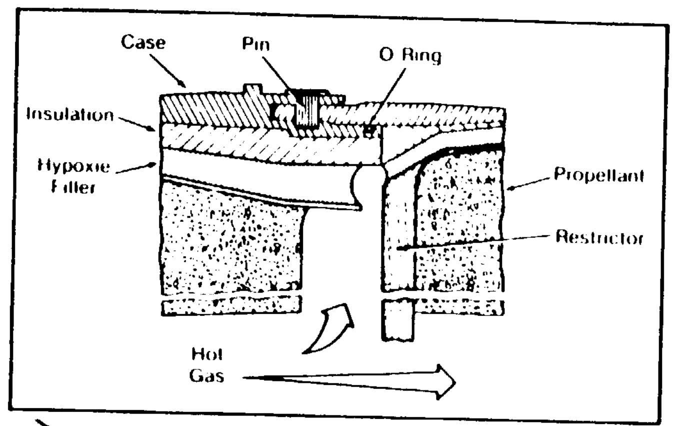

STS Joint Detail

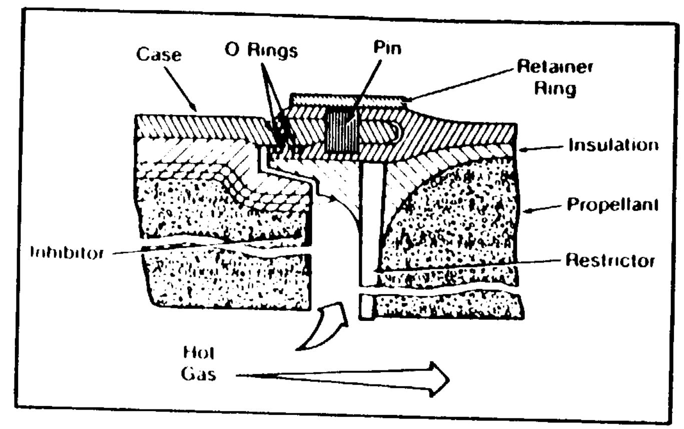

34D Cylinder Geometry

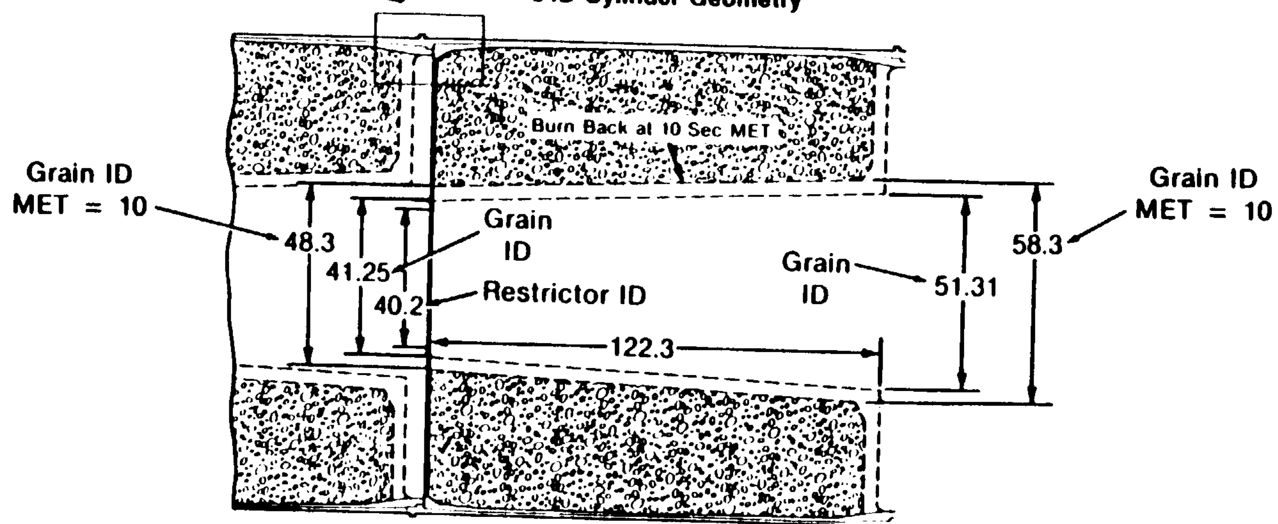

Notes:

- As Fabricated Dimensions (Inches) Are Shown for Titan 34D-9 Per Written Record of Conference Call Cork, Spitale, and Eck With S. Backlund United Technology Corp 12 Oct 87
- 34D Grain Is One Cylinder Long
- STS Grain Is Two Cylinders Long (~300 Inches) and Essentially Untapered

S-087 61R 07 88C

EFFECT OF FLOW INTO THE CASING-GRAIN CAVITY FROM AN UNSPECIFIED LONGITUDINAL FLOW PATH ON RIGID-BODY-MODEL PREDICTED 34D-9 SRM FRAGMENT VELOCITY

Ratio of 3D Bypass Flow Area to Burn Area	Casing Fragment Velocity m/s	Grain Fragment Velocity m/s
0	85	30
0.001	85	30
0.01	89	28
0.02	94	26
0.04	104	23
0.08	120	17
0.16	140	8
0.20	146	5
0.40	157	1
0.50	158	0
1.00	162	0

CONCLUSION:

A single chamber flow model can be justified if a grain flow channel bypass path with a flow area equal to 40 percent of the grain ID area can be identified. Such a model will produce unrealistically low grain fragment velocities.

S-087.83 02-89C

NORMALIZED CAVITY AND CHAMBER PRESSURE AS A FUNCTION OF TIME AFTER LSC INITIATION

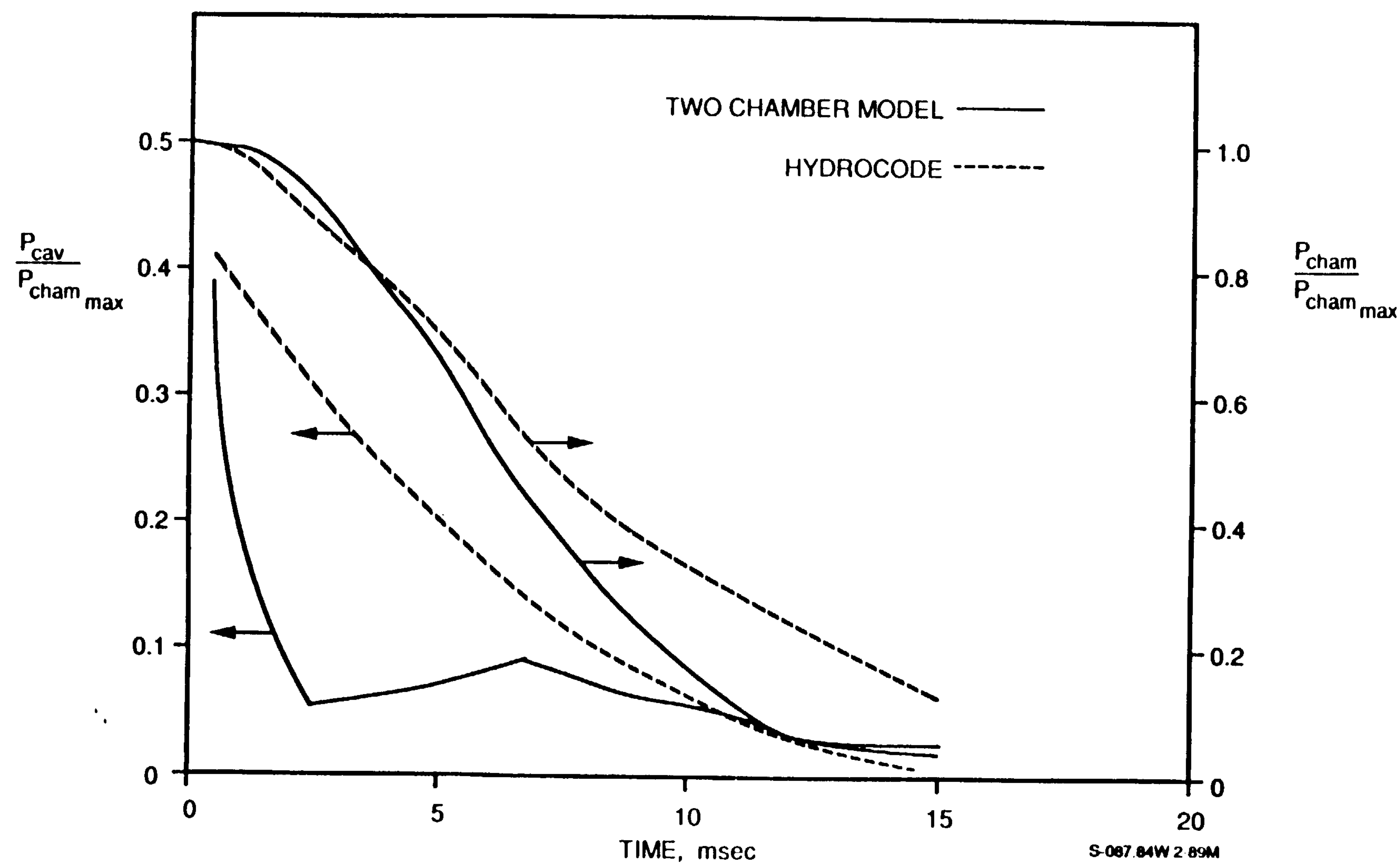

SUMMARY OF RESULTS OBTAINED FROM THE RIGID BODY MODELS OF STS EVENTS

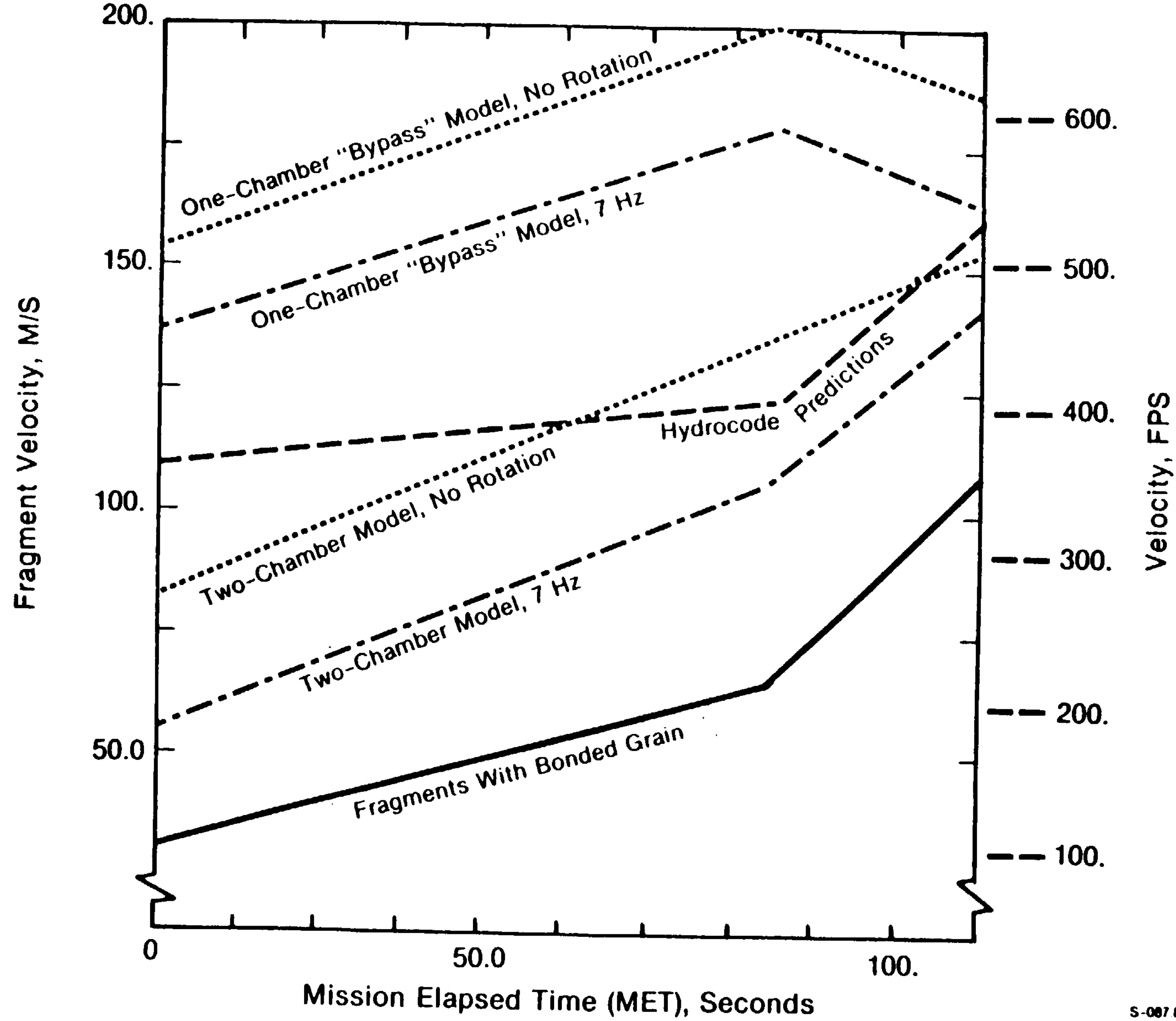

S-087 85R 02-89C

MODEL BOUNDARY ASSUMPTION VERIFICATION

- A NUMBER OF BOUNDARY ASSUMPTIONS WERE MADE IN THE VARIOUS MODELS USED TO DEVELOP THE SHUTTLE DATA BOOK DATA BASE.
- VARIOUS INVESTIGATORS CALLED MANY OF THESE ASSUMPTIONS INTO QUESTION.
- A TASK WAS INITIATED TO TEST THE ASSUMPTIONS UPON WHICH THE MODELS WERE BASED.
- CENTRAL TO THIS TASK WAS ESTABLISHING THE BEHAVIOR OF THE GRAIN DURING THE PERIOD AFTER THE CASING FAILED AND BEFORE CHAMBER GAS BEGAN TO VENT.
- DETAILED MODELING OF GRAIN AND GRAIN CRACK PROPAGATION WAS UNDERTAKEN TO ANSWER QUESTIONS ABOUT THE RELATIVE IMPORTANCE OF MATERIAL INERTIA AND STRENGTH.
- A COMPLETELY NEW 2D AXISYMMETRICAL COUPLED EULERIAN-LAGRANGIAN MODEL WAS DEVELOPED FOR THIS TASK.

MODEL BOUNDARY ASSUMPTION VERIFICATION (CONT'D)

- THE NEW MODEL HAD THE FOLLOWING FEATURES:
  - LOCATIONS WHERE CRACKS COULD INITIATE AND PROPAGATE THRU THE GRAIN.
  - CRACK INITIATION WAS BASED ON A LOCAL STRAIN TO FAILURE CRITERION.
  - ONLY TEN POTENTIAL CRACK LOCATIONS COULD BE CHOSEN BECAUSE OF CODE ARRAY LIMITATIONS.
  - CASING-GRAIN BOND STRENGTH PRIOR TO DEBONDING WAS MODELED.
  - GRAIN STRENGTH PRIOR TO GRAIN FRACTURE WAS MODELED.
  - EQUILIBRIUM STRESSES WERE ESTABLISHED USING LOW STRAIN RATE MATERIAL PROPERTIES.
  - HIGH STRAIN RATE PROPERTIES WERE INTRODUCED AS HIGH RATES DEVELOPED.
  - THE MASS OF THE PBAN GAS STORED IN THE CHAMBER AT 10 SEC MET IS FIVE TIMES GREATER THAN THE MASS GENERATED BY BURNING FOR 20 MSEC AT 60 BARS.

MODEL BOUNDARY ASSUMPTION VERIFICATION (CONT'D)

- NO ENHANCED BURNING WAS USED TO INCREASE CHAMBER ENERGY DURING THE ~30 MSEC REQUIRED TO COMPLETE THE BLOW DOWN PROCESS.

- LOCAL TOTAL STRAIN AT THE 10 JOINED LAGRANGIAN SUBGRID LOCATIONS WAS MONITORED AUTOMATICALLY AND THE RUN WAS STOPPED WHEN TOTAL STRAIN EXCEEDED 30 PERCENT.

- DEFECTS WERE INTRODUCED INTO THE GRAIN BY REMOVING THE JOINS BETWEEN ADJACENT SUBGRIDS.

- IF THE DEFECTS COULD COMMUNICATE WITH THE HOT GAS, CHAMBER PRESSURE WAS APPLIED TO THE SEPARATED SURFACES GENERATED BY THE CRACK.

- THE RUN WAS RESTARTED AND THE PROCESS OF MANUALLY REMOVING SUBGRID JOINS WAS CONTINUED UNTIL A CRACK PROPAGATED THRU THE GRAIN.

- CASING AND GRAIN MOTIONS, STRAIN STATES, AND RATES WERE TRACKED UNTIL CHAMBER PRESSURE DISSIPATED.

- THE RESULTS OBTAINED USING THIS PROCESS ARE SHOWN IN THE FOLLOWING VUGRAPHS.

TIME LINE FOR A STS-SRM SEGMENT RESPONSE TO A RANGE SAFETY DESTRUCT ACTION AT 10 sec MET

Time msec	Event
0	Linear shaped charge fired. PBAN cut 12 cm deep at 0°.
1.2	Debond failure strain reaches 45° and crack initiates on grain external diameter (OD).
6.2	Debond failure strain reaches 90° and crack initiates on grain OD.
12.1	Debond failure strain reaches 135° and first crack initiates in grain internal diameter (ID) at GR2/GR3 interface.
12.4	Crack initiates in grain ID at GR3/GR4 and GR9/GR10 interfaces.
13.3	Crack initiates at cut-line ID (GR1/GR10 interface).
14.6	Crack initiates at GR5/GR6 interface and at GR7/GR8 interface by symmetry.
23.4	First crack has traversed grain at GR3/GR4 interface.
23.9	Grain cracks thru at GR1/GR10 interface.
26.1	Grain cracks thru at GR2/GR3 interface.
26.5	Grain cracks thru at GR9/GR10 interface.

S-087.86 02-89C

VARIATION OF THE SQUARE ROOT OF THREE TIMES THE SECOND INVARIANT OF THE STRESS DEVIATOR TENSOR

$$J_2' = \tfrac{1}{2}\left(S_{xx}^2 + S_{yy}^2 + 2S_{xy}^2\right);\ \text{YIELD} = \left(3J_2'\right)^{1/2} \equiv 48.3\ \text{BARS}$$

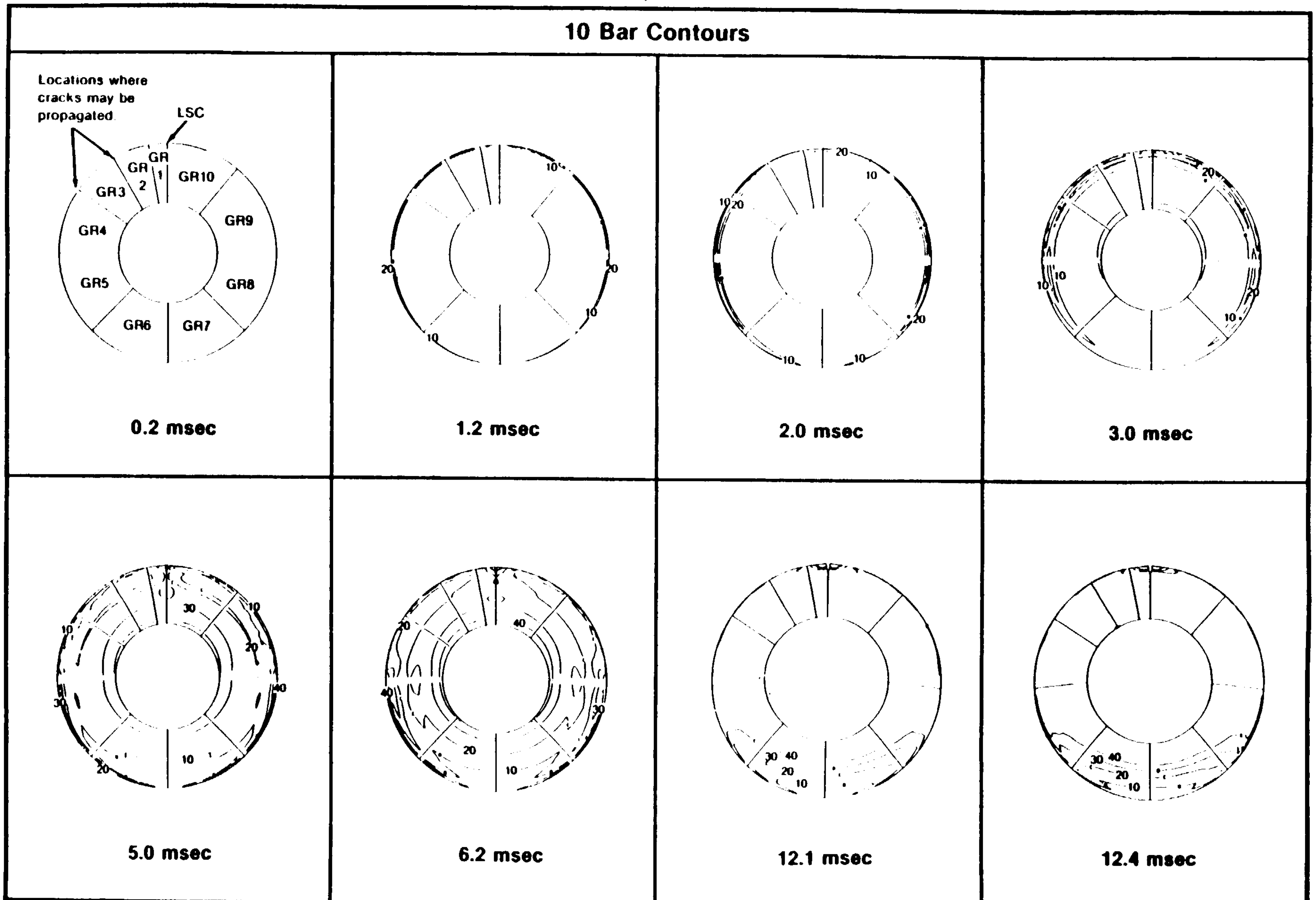

S-087.91R 02-89C

VARIATION OF THE SQUARE ROOT OF THREE TIMES THE SECOND INVARIANT OF THE STRESS DEVIATOR TENSOR

$J_2' = \frac{1}{2}(S_{xx}^2 + S_{yy}^2 + 2S_{xy}^2)$; YIELD $= (3J_2')^{1/2} \equiv 48.3$ BARS

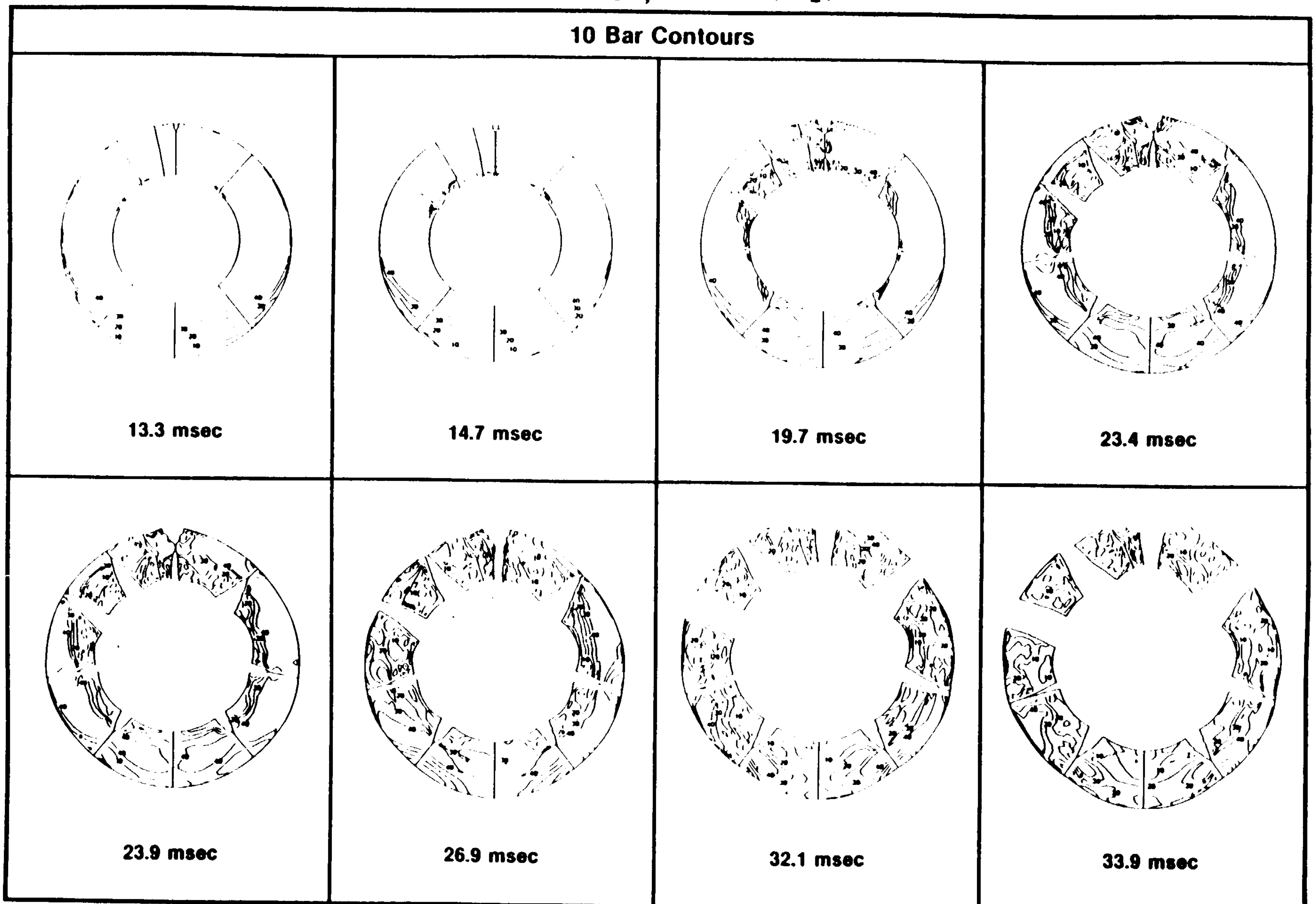

S-087 92R 02 89C

VARIATION OF RESULTANT STRAIN RATE ($\dot{\epsilon}$) WITH TIME AFTER LSC INITIATION

$$\dot{\epsilon} = 2/3(\dot{\epsilon}_{xx} + \dot{\epsilon}_{yy} + 2\,\dot{\epsilon}_{xy})^{1/2}$$

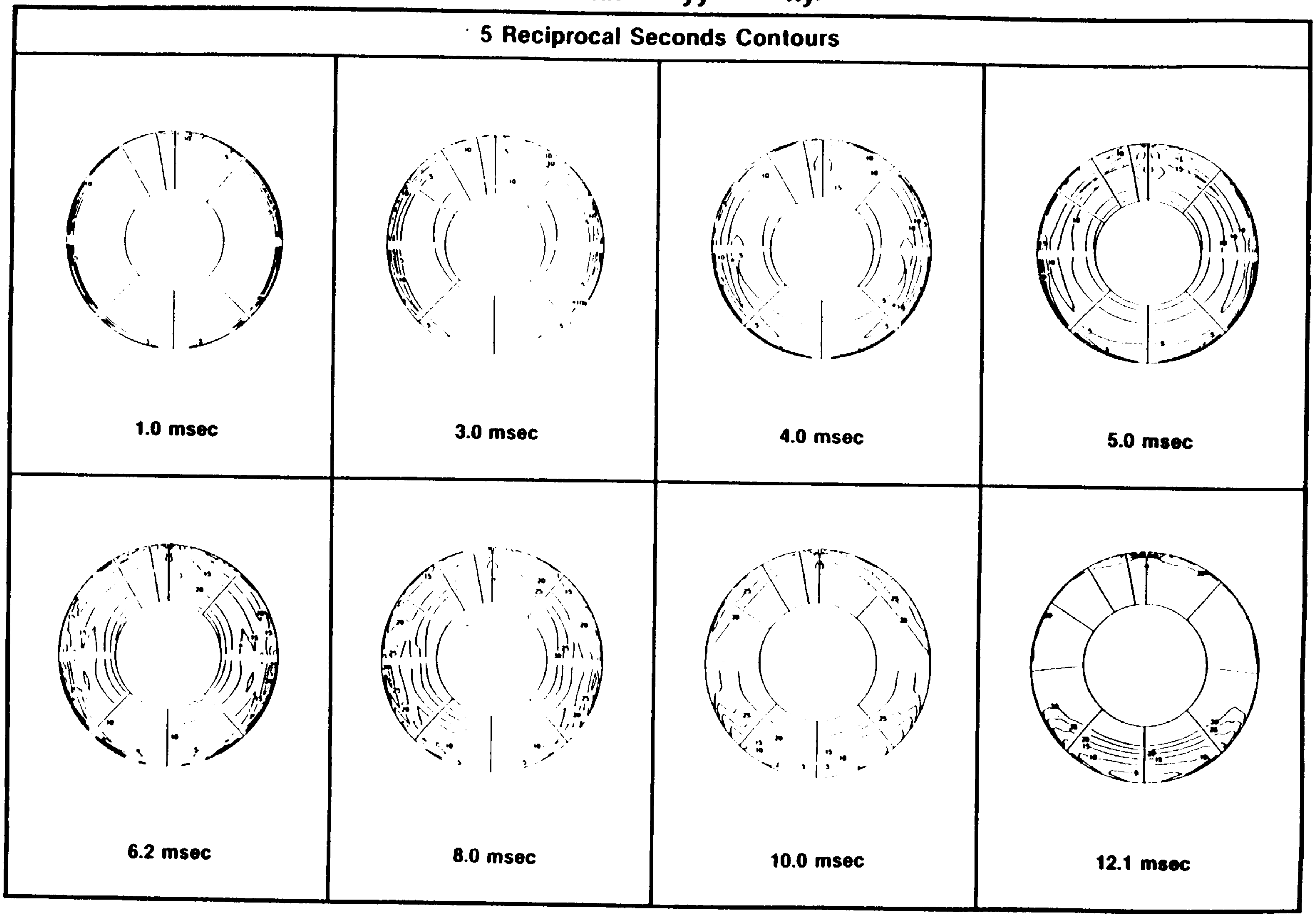

S-087.103R 02-89C

VARIATION OF RESULTANT STRAIN RATE ($\dot{\epsilon}$) WITH TIME AFTER LSC INITIATION

$$\dot{\epsilon} = 2/3(\dot{\epsilon}_{xx} + \dot{\epsilon}_{yy} + 2\,\dot{\epsilon}_{xy})^{1/2}$$

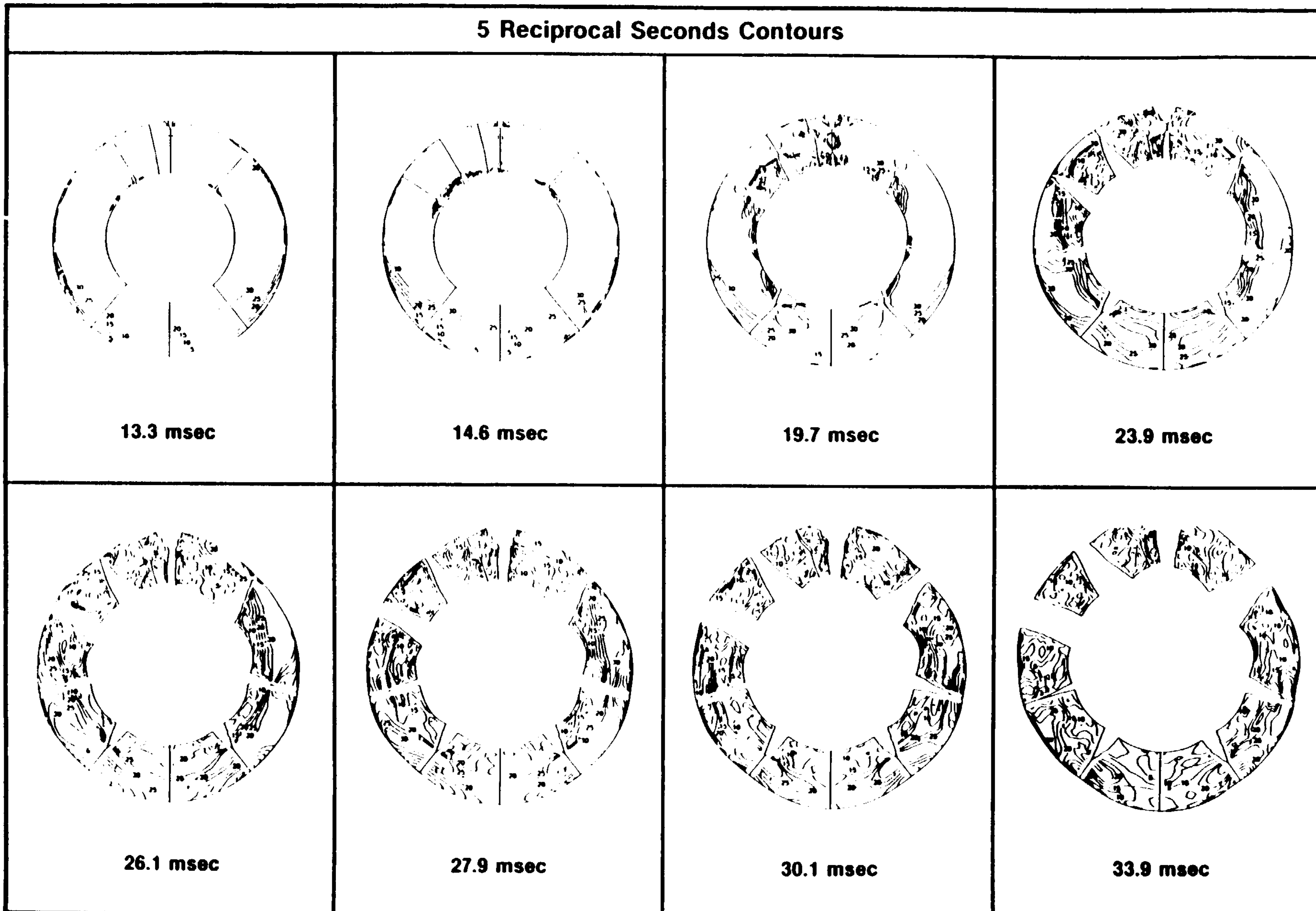

S-087.102R 02-89C

GRAIN TOTAL STRAIN AS A FUNCTION OF TIME

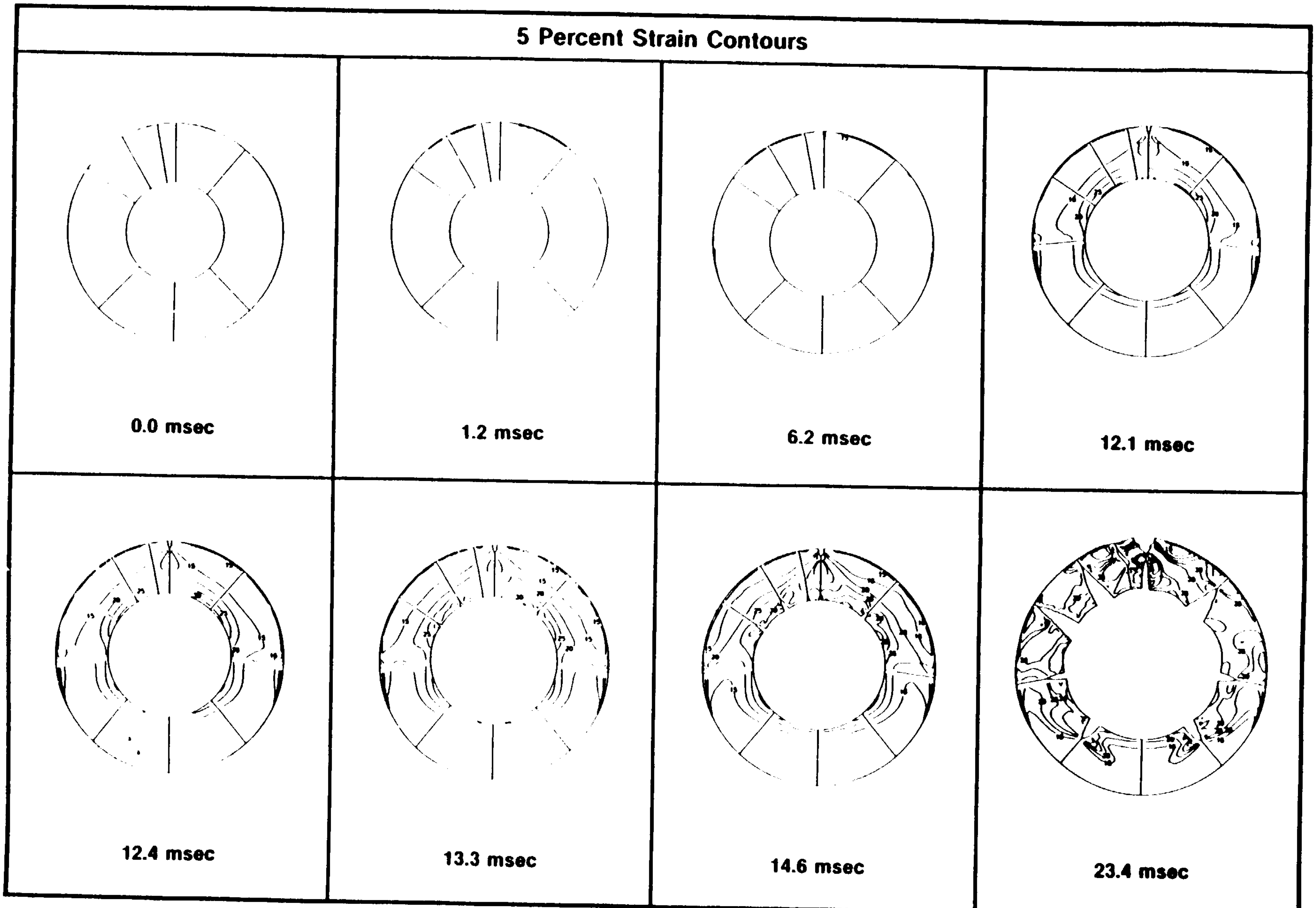

S-087.89R 02-89C

RELATIVE CASING AND GRAIN GEOMETRY AS A FUNCTION OF TIME AFTER THE RSD OF AN STS-SRM AT 10 SEC MET

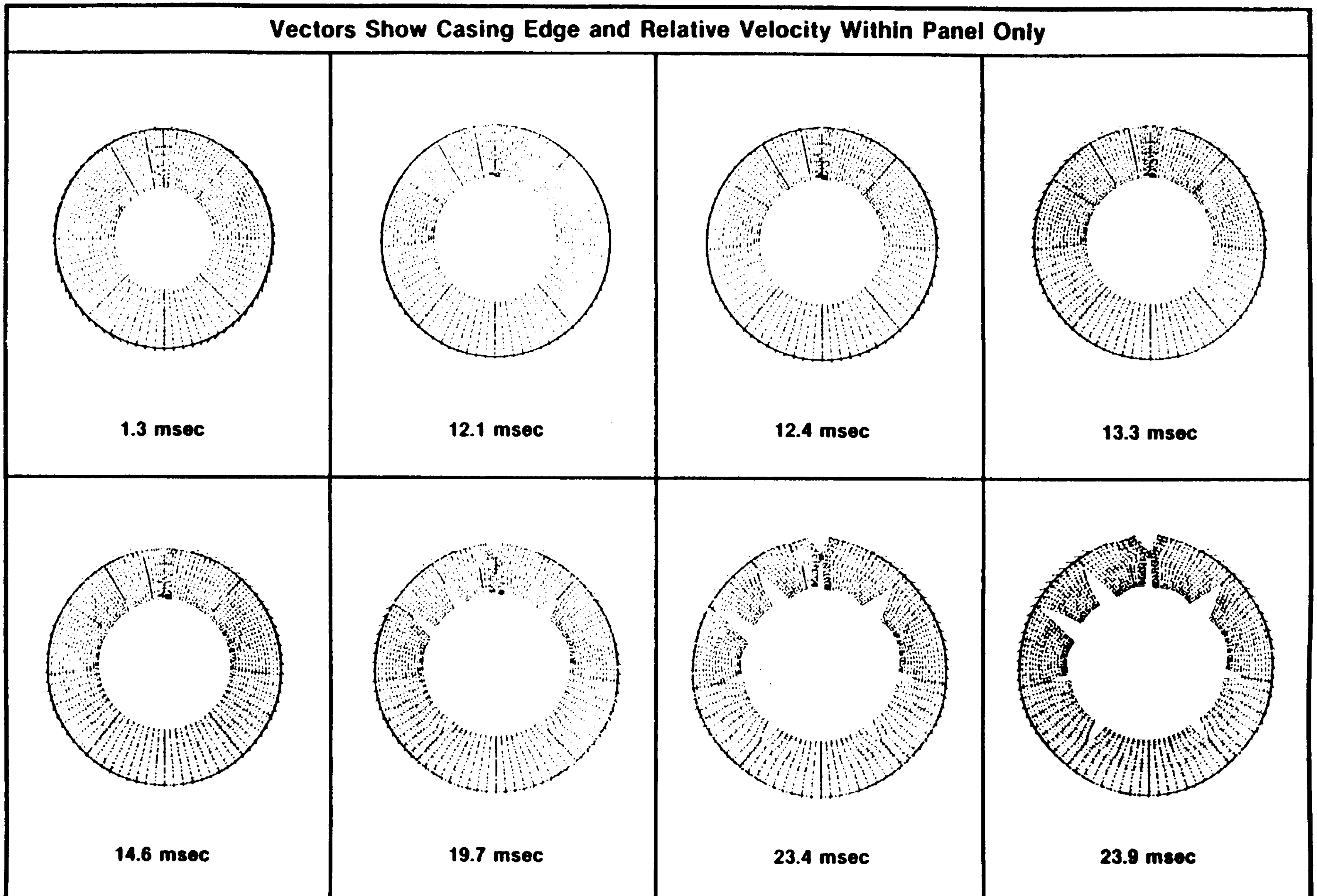

S-087 93R 02 89C

RELATIVE CASING AND GRAIN GEOMETRY AS A FUNCTION OF TIME AFTER THE RSD OF AN STS-SRM AT 10 SEC MET

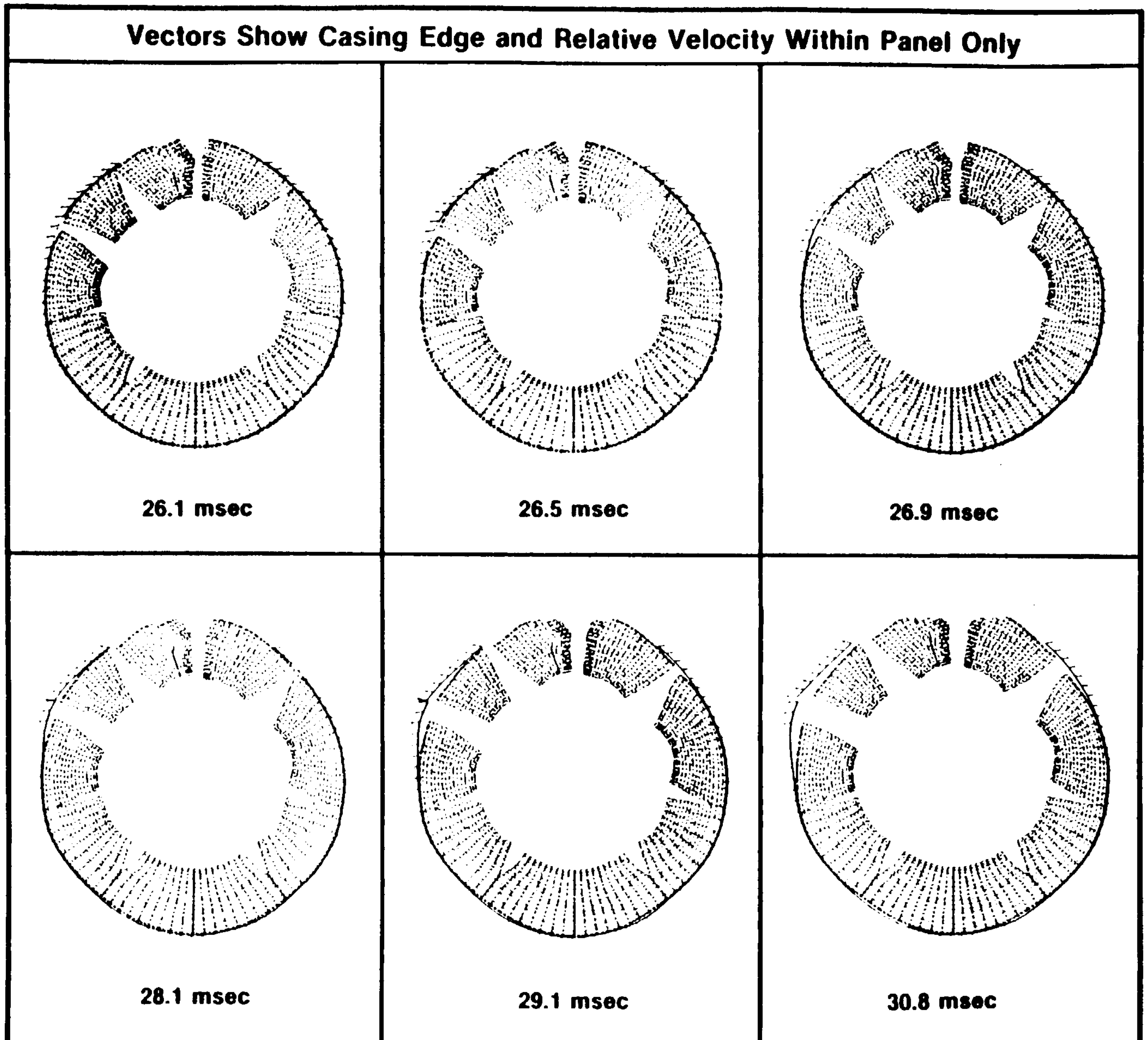

S-087 90R 02-89C

DEVELOPING FLOW FIELD IN THE GRAIN - CASING CAVITY AT VARIOUS TIMES AFTER A STS-SRM CASING FAILURE AT 10 SECONDS MET

CASING FRAGMENTATION AT 26.9 MSEC